Title: Closed universes and the CMB / Spin-SILC: CMB polarisation component separation for next-generation experiments

Date: Aug 04, 2016 11:00 AM

URL: http://pirsa.org/16080032

Abstract: 1. Beatrice Bonga, "Closed universes and the CMB",

Abstract:
Cosmic microwave background (CMB) observations put strong constraints on the spatial curvature via estimation of the parameter Ω_k. This is done assuming a nearly scale-invariant primordial power spectrum. However, we found that the inflationary dynamics is modified due to the presence of spatial curvature leading to corrections to the primordial power spectrum. When evolved to the surface of last scattering, the resulting temperature anisotropy spectrum shows deficit of power at low multipoles ($\ell<20$). This may partially explain the observed 3σ anomaly of power suppression for $\ell <30$. Since the curvature effects are limited to low multipoles, the estimation of cosmological parameters remains robust under inclusion of positive spatial curvature.

(This talk is based on http://arxiv.org/abs/1605.07556)

2. Keir Rogers, "Spin-SILC: CMB polarisation component separation for next-generation experiments",

Abstract:

B-mode polarisation is a powerful cosmological observable which in principle allows the detection of a stochastic background of gravitational waves predicted by inflation, and gives strong constraints on the neutrino sector using the weak gravitational lensing of the cosmic microwave background (CMB). Astrophysical foregrounds present a formidable obstacle in extracting these signatures of new physics from CMB polarisation data. Indeed, recent forecasts for post-2020 CMB experiments predict one sigma constraints on, for example, the tensor-to-scalar ratio of about 10^-4 and the sum of neutrino masses of about 30 meV. However, these constraints are predicated on highly-accurate foreground and noise removal. I will present the first component separation method specifically developed for this task and tested on the latest-release Planck data. The method, Spin-SILC, is an internal linear combination algorithm that uses spin wavelets to fully analyse the spin polarisation signal P = Q + iU, where Q and U are the measured Stokes parameters. This allows all the information in the measured signal to be used in extracting the cosmological background. Furthermore, Spin-SILC is the first method to simultaneously and efficiently perform component separation and the E-B decomposition necessary for cosmological analyses thanks to the construction of the spin wavelets we use. Spin-SILC also uses the morphological information of the foregrounds and CMB to better localise the cleaning algorithm. This is because the wavelets we use are additionally directional, and, when convolved with signals on the sphere, can separate the filamentary structures which are characteristic of both the CMB and foregrounds. I will present the results of applying these novelties to Planck data and discuss further how Spin-SILC can also mitigate the E-B leakage problem of future CMB experiments.

ΛCDM + inflation

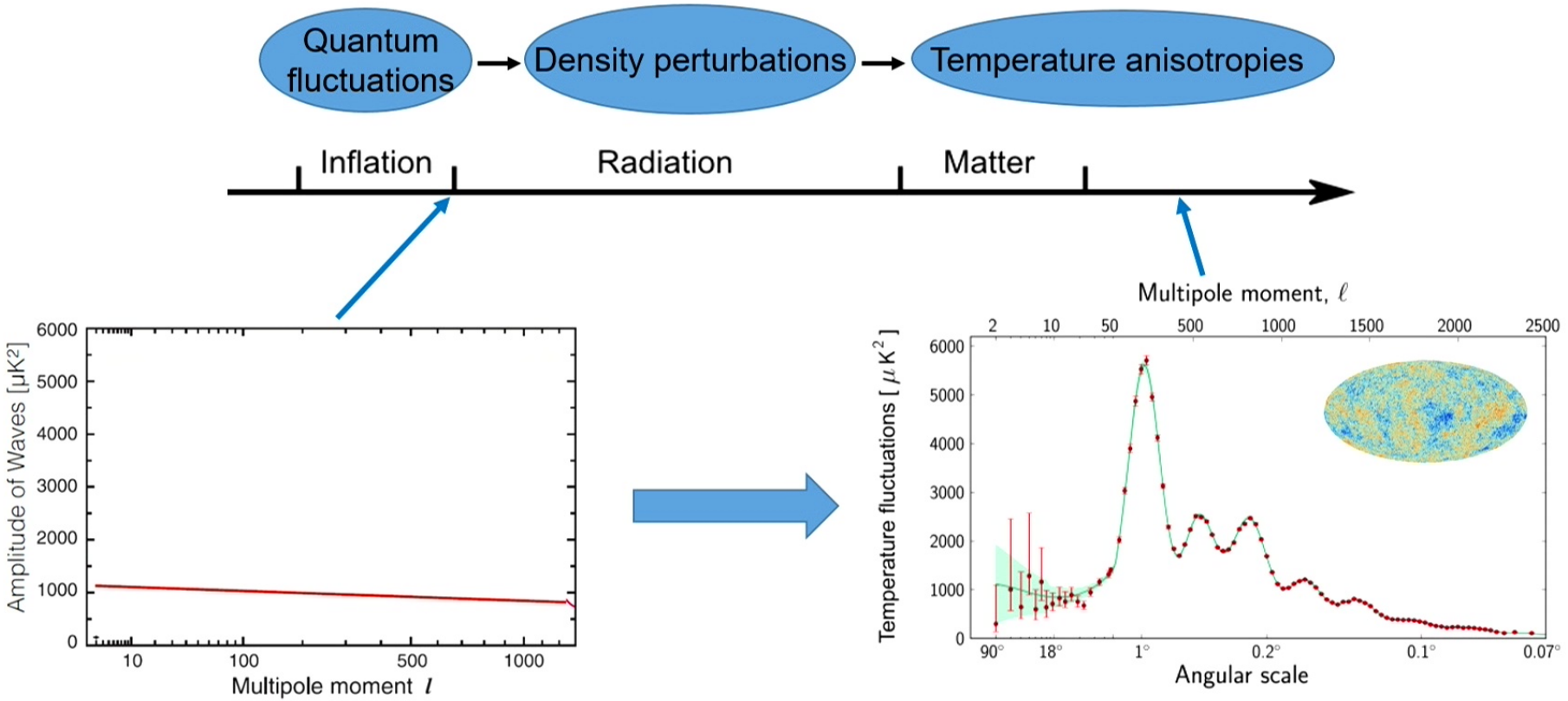

$$\Omega_K = -\frac{\rho_k}{\frac{3}{8\pi G}H_0^2}$$

Constraining spatial curvature

Planck

$\Omega_K = -0.005^{+0.016}_{-0.017}$

Planck + BAO

$\Omega_K = 0.000^{+0.005}_{-0.005}$

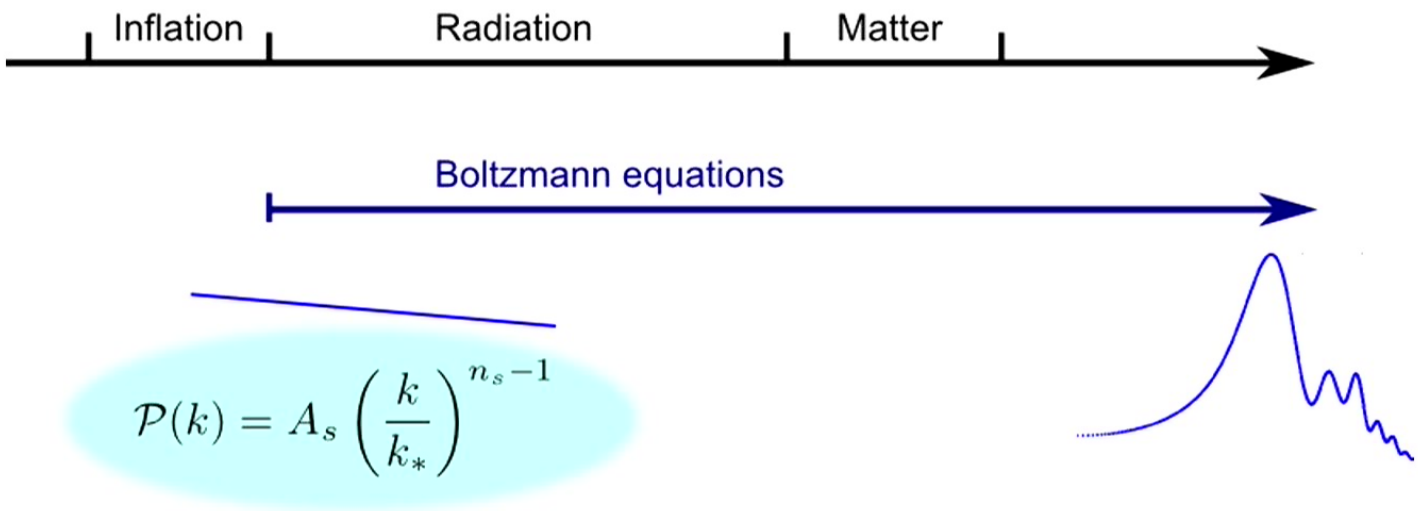

$$\Omega_K = -\frac{\rho_k}{\frac{3}{8\pi G}H_0^2}$$

Constraining spatial curvature

Planck

$\Omega_K = -0.005^{+0.016}_{-0.017}$

Planck + BAO

$\Omega_K = 0.000^{+0.005}_{-0.005}$

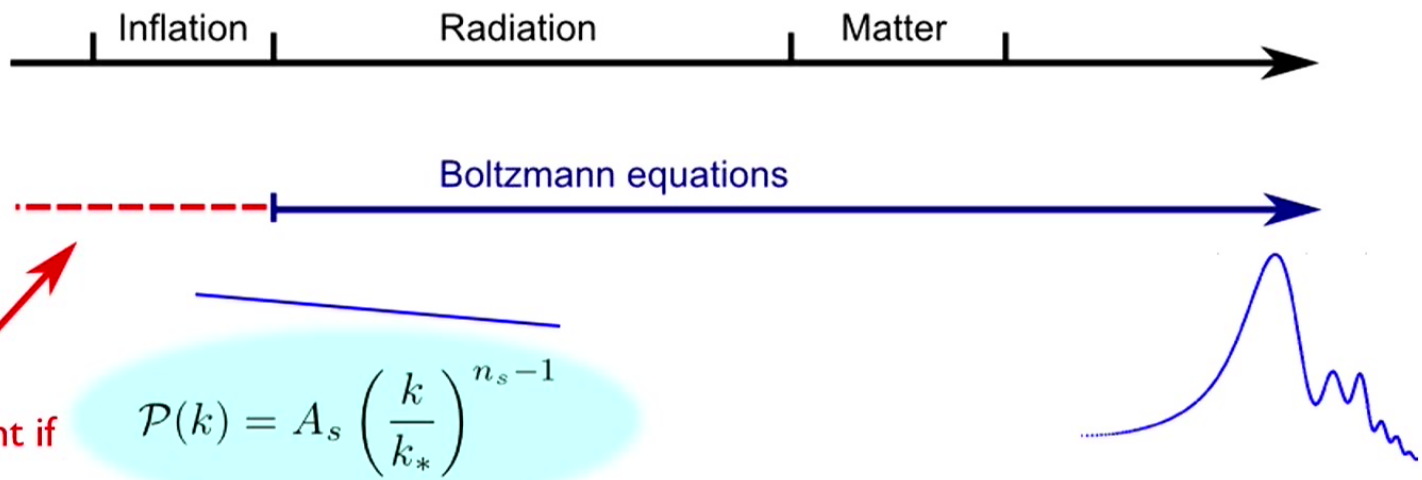

$$\mathcal{P}(k) = A_s \left(\frac{k}{k_*}\right)^{n_s - 1}$$

Is this consistent if there is spatial curvature?

Previous work

1. Implementation in Boltzmann equations (and codes) [Lewis, Challinor, Lasenby]

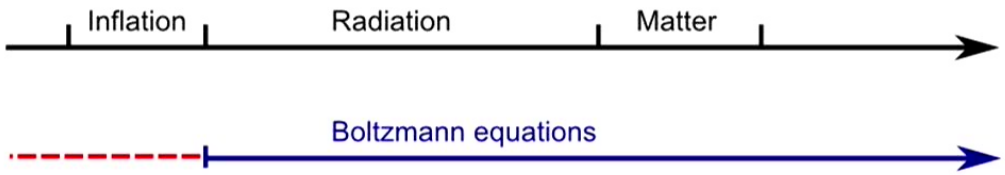

2. Inflation in the context of closed model [Linde; Doran, Lasenby; Ellis, Stoerger, McEwan, Dunsby; Efstathiou; White, Scott; Uzan, Kirchner, Ellis]

3. Effects on curvature perturbation using approximate methods [Masso, Mchanty, Nautiyal, Zsembinski]

Questions

1. Does spatial curvature modify the primordial power spectrum?

2. Implications for CMB? And for estimation of Ω_K?

Outline

- Background
- Gauge-invariant perturbations
- Results
- Outlook

Why you should care

$$H^2 = H_0^2 \left(\Omega_{\rm m} \left(\frac{a}{a_0} \right)^{-3} + \Omega_{\rm r} \left(\frac{a}{a_0} \right)^{-4} + \Omega_\Lambda + \Omega_{\rm k} \left(\frac{a}{a_0} \right)^{-2} \right)$$

$$\left. \frac{\rho_{\rm k}}{\rho_{\rm r}} \right|_{\rm beg\ rad} \approx 10^{-57} \approx \left. \frac{\rho_{\rm k}}{\rho_\phi} \right|_{\rm end\ inf}$$

Why you should care

$$H^2 = H_0^2 \left(\Omega_{\rm m} \left(\frac{a}{a_0} \right)^{-3} + \Omega_{\rm r} \left(\frac{a}{a_0} \right)^{-4} + \Omega_\Lambda + \Omega_{\rm k} \left(\frac{a}{a_0} \right)^{-2} \right)$$

$$\left. \frac{\rho_{\rm k}}{\rho_{\rm r}} \right|_{\rm beg\ rad} \approx 10^{-57} \approx \left. \frac{\rho_{\rm k}}{\rho_\phi} \right|_{\rm end\ inf}$$

However, ~60 e-folds before end of inflation curvature does become important!

Set up in ADM formalism

Truncated phase space: $\Gamma = \Gamma_0 \times \Gamma_1$

Background phase space $\Gamma_0(a, \phi; \pi_a, \pi_\phi)$

- Dynamics generated by background Hamiltonian

Background during inflation

$$H^2 = \frac{8\pi G}{3}\left(\rho_\phi - \frac{\rho_k}{a^2}\right)$$

$$\ddot{\phi} + 3H\dot{\phi} + \frac{dV}{d\phi} = 0$$

Two potentials: quadratic and Starobinsky

Background during inflation

$$H^2 = \frac{8\pi G}{3}\left(\rho_\phi - \frac{\rho_k}{a^2}\right)$$

limits max # e-folds

$$\ddot{\phi} + 3H\dot{\phi} + \frac{dV}{d\phi} = 0$$

Two potentials: quadratic and Starobinsky

Potentials

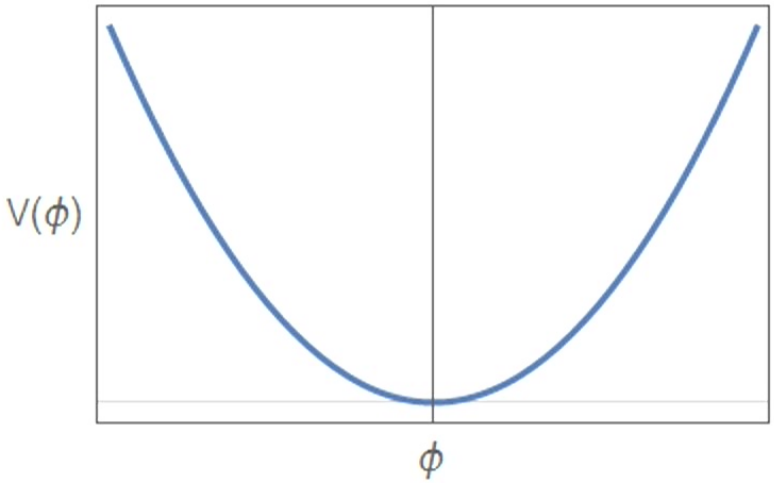

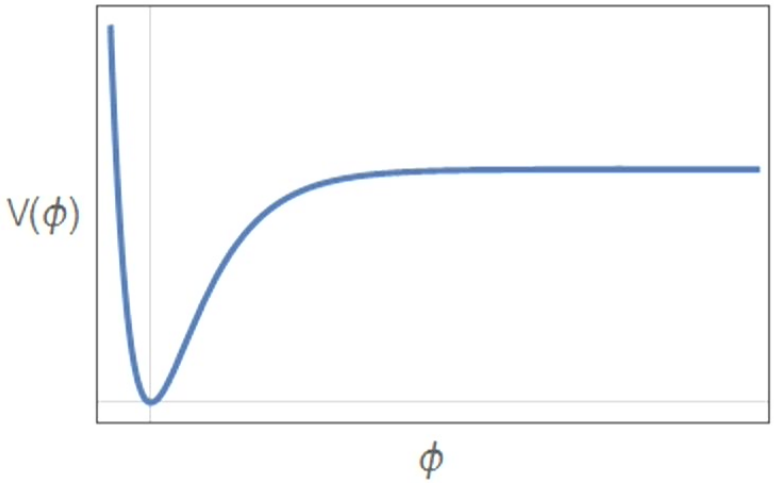

$$V(\phi) = \frac{1}{2}m^2\phi^2$$

$$V(\phi) = \frac{3M^2}{32\pi G}\left(1 - e^{-\sqrt{\frac{16\pi G}{3}}\phi}\right)^2$$

Initial conditions background

Use input Planck:

- Amplitude scalar power spectrum $A_s \pm 2\ \sigma_{A_s}$
- Spectral index $n_s \pm 2\ \sigma_{n_s}$

Einstein's equations

Quadratic

$\phi = 2.99 \pm 0.52\ m_{\rm Pl}$, $\quad \dot{\phi} = (-2.08 \pm 0.73) \times 10^{-7}\ m_{\rm Pl}^2$

$a = (3.3 \pm 0.6) \times 10^{-54} \quad m = (1.28 \pm 0.45) \times 10^{-6}\ m_{\rm Pl}$

Starobinsky

$\phi = 1.08 \pm 0.02\ m_{\rm Pl}$, $\quad \dot{\phi} = (-4.80 \pm 0.70) \times 10^{-9} m_{\rm Pl}^2$

$a = 2.11 \pm 0.14 \times 10^{-53} \quad M = (2.56 \pm 0.18) \times 10^{-6}\ m_{\rm Pl}$

Comoving Hubble radius

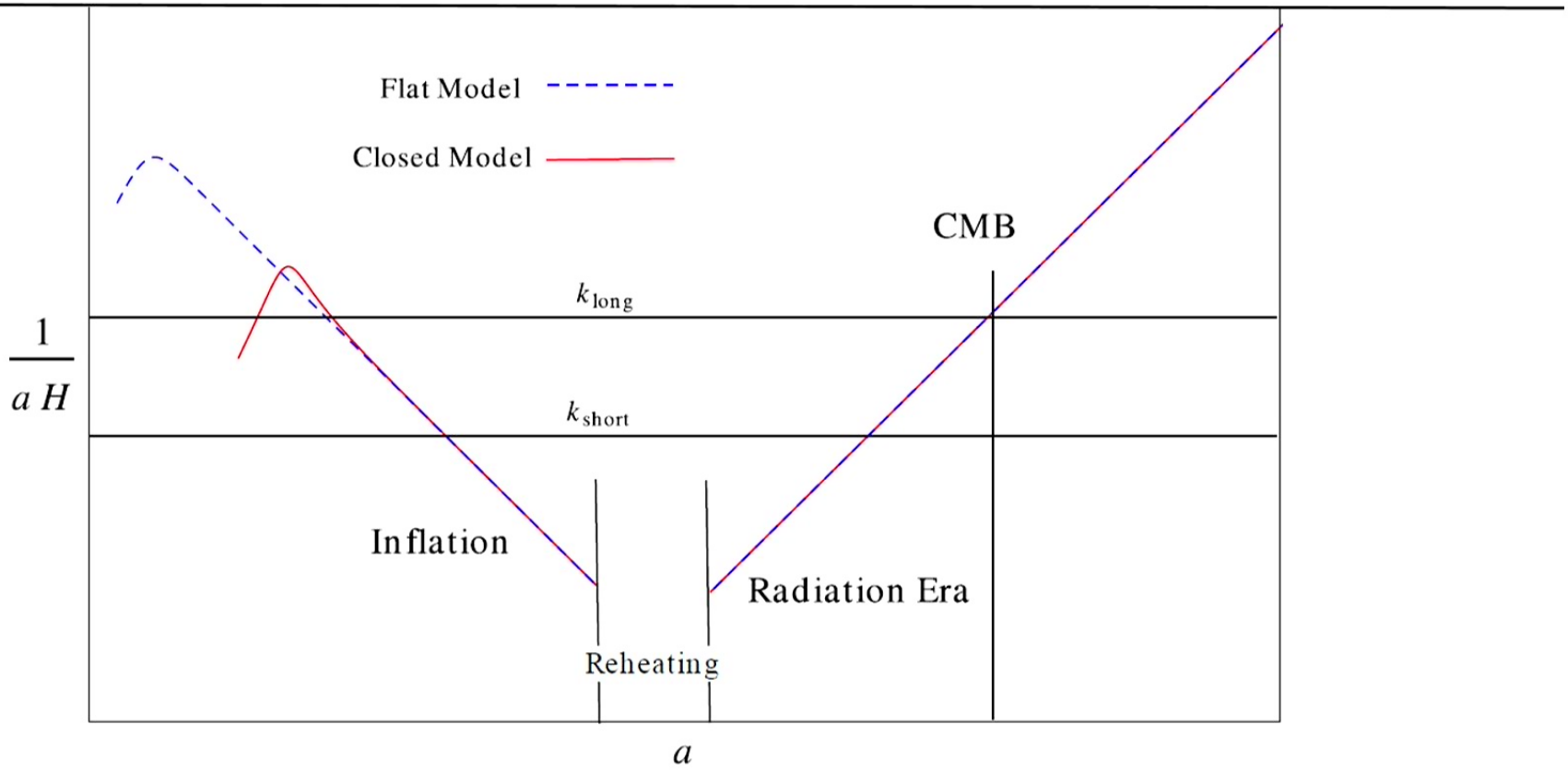

Set up in ADM formalism

Truncated phase space: $\Gamma = \Gamma_0 \times \Gamma_1$

Background phase space $\Gamma_0(a, \phi; \pi_a, \pi_\phi)$

- Dynamics generated by background Hamiltonian

Linearized phase space $\Gamma_1(\gamma_1, \gamma_2, \delta\phi; \pi_1, \pi_2, \pi_{\delta\phi})$

- Linearized Hamiltonian and diffeomorphism are constraints

$$\Rightarrow Q = \delta\phi - \sqrt{\mathcal{V}_0}\frac{\dot{\phi}}{H}(\gamma_1 + \gamma_2) \left(= \frac{\dot{\phi}}{H}\zeta\right)$$

- Dynamics generated Hamiltonian quadratic in perturbations

Hyperspherical harmonics

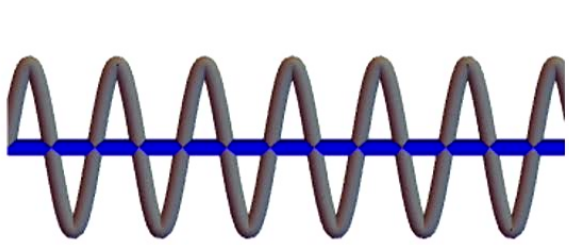

$\mathbb{R}$

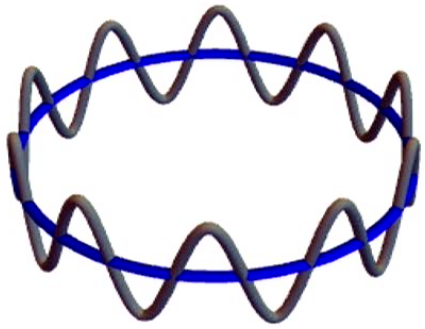

$\mathbb{S}$

Plane waves

Hyperspherical harmonics

$$Q(t,\vec{x}) = \int dk\, k^2 \sum_{l=0}^{n-1} \sum_{m=-l}^{l} q_{klm}(t)\, j_l(kr) Y_{lm}(\theta,\phi)$$

$$Q(t,\vec{x}) = \sum_{n=2}^{\infty} \sum_{l=0}^{n-1} \sum_{m=-l}^{l} q_{nlm}(t)\, \mathcal{Q}_{nlm}(\vec{x})$$

$$\frac{k^2}{a^2_{\text{flat}}(t)} = \frac{n^2-1}{a^2_{\text{closed}}(t)}$$

Dynamics

Generated by Hamiltonian quadratic in gauge-invariant perturbations

$$\ddot{q}_{nlm} + b(n,t)\dot{q}_{nlm} + c(n,t)q_{nlm} = 0$$

$$b \xrightarrow{\text{dS}} 3H$$

$$c \xrightarrow{\text{dS}} -\frac{n^2-1}{r_o^2\, a^2}$$

Dynamics

Generated by Hamiltonian quadratic in gauge-invariant perturbations

$$\ddot{q}_{nlm} + b(n,t)\dot{q}_{nlm} + c(n,t)q_{nlm} = 0$$

$$b \xrightarrow{\text{dS}} 3H \qquad c \xrightarrow{\text{dS}} -\frac{n^2-1}{r_o^2\, a^2}$$

$$b \xrightarrow{\text{flat}} 3H \qquad c \xrightarrow{\text{flat}} -\frac{k^2}{a^2} + \mathcal{U}$$

b(n,t) & c(n,t)

$$b(n,t) \;=\; 3H \;+\; \frac{32\pi G a^3 \dot{a}\dot{\phi}V'(\phi) + 48\pi G a^2 \dot{a}^2\dot{\phi}^2 - 8\pi G a^2\dot{\phi}^2\left(8\pi G a^2\left(\dot{\phi}^2 - 2V\right)+2\right)}{2a\dot{a}\left(2(n^2-4)\dot{a}^2 + 8\pi G a^2\dot{\phi}^2\right)}$$

$$c(n,t) = \frac{8\pi G}{a^2\dot{a}^2\left(2\left(n^2-4\right)\dot{a}^2 + 8\pi G a^2\dot{\phi}^2\right)}$$

$$\left[\frac{\dot{a}^4(n^2-4)\left(n^2-1+a^2V''\right)}{4\pi G} + \left(4n^2-7\right)a^3\dot{a}^3\dot{\phi}V' - \pi G\frac{n^2-1}{n^2-4}a^4\dot{\phi}^4\left[8\pi G a^2\left(\dot{\phi}^2+2V\right)-6\right]\right.$$

$$+ (n^2-1)a^2\dot{a}^2\left(-6\pi G\frac{n^2-5}{n^2-4}a^2\dot{\phi}^4 + 4\pi G a^2\dot{\phi}^2V + \frac{3}{2}\dot{\phi}^2 + \frac{9}{2}\dot{a}^2\dot{\phi}^2\right)$$

$$\left. + a^3\dot{a}\left[a\dot{a}\dot{\phi}^2V'' + 2a\dot{a}V'^2 + 4\pi G a^2\dot{\phi}V'\left(\dot{\phi}^2+2V\right) - \dot{\phi}V'\right]\right]$$

b(n,t) for n=3 and n=20

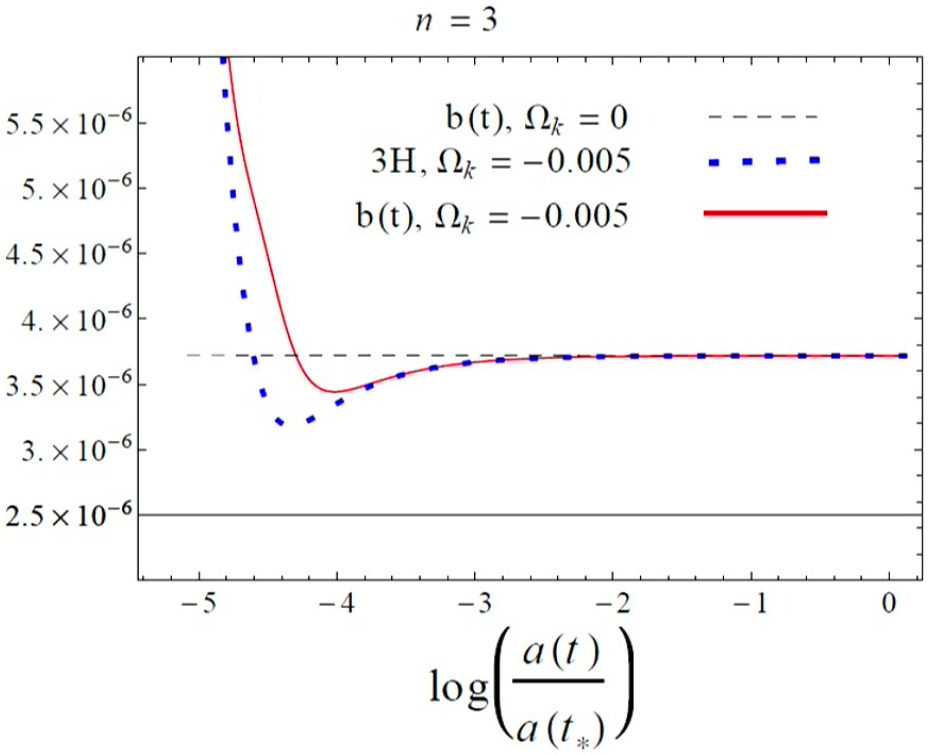

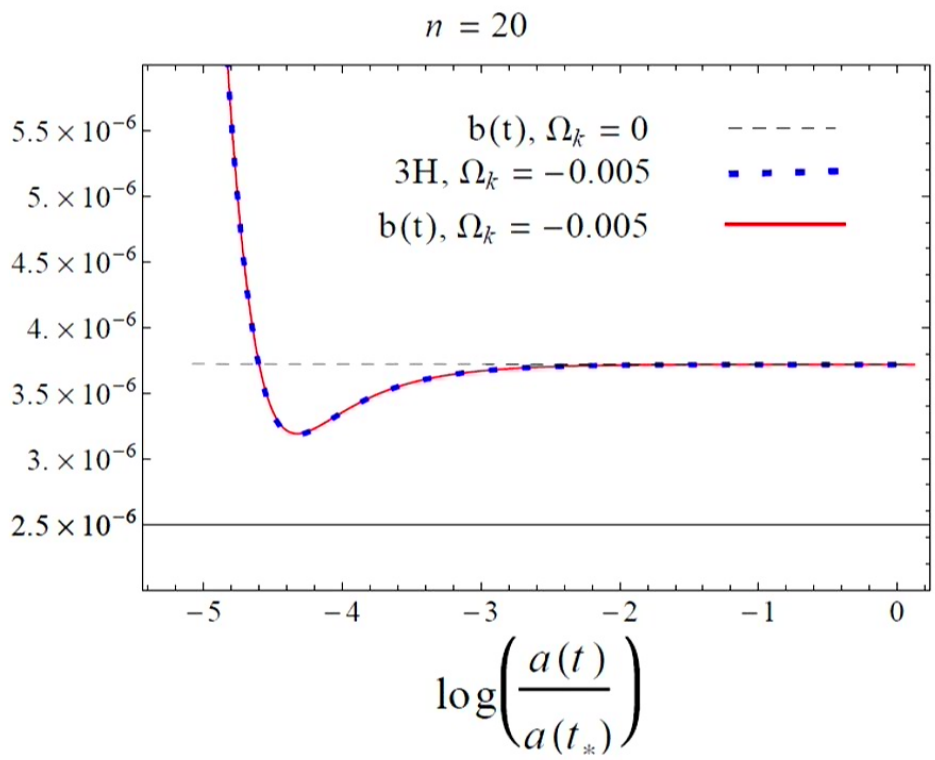

b(n,t) for n=3 and n=20

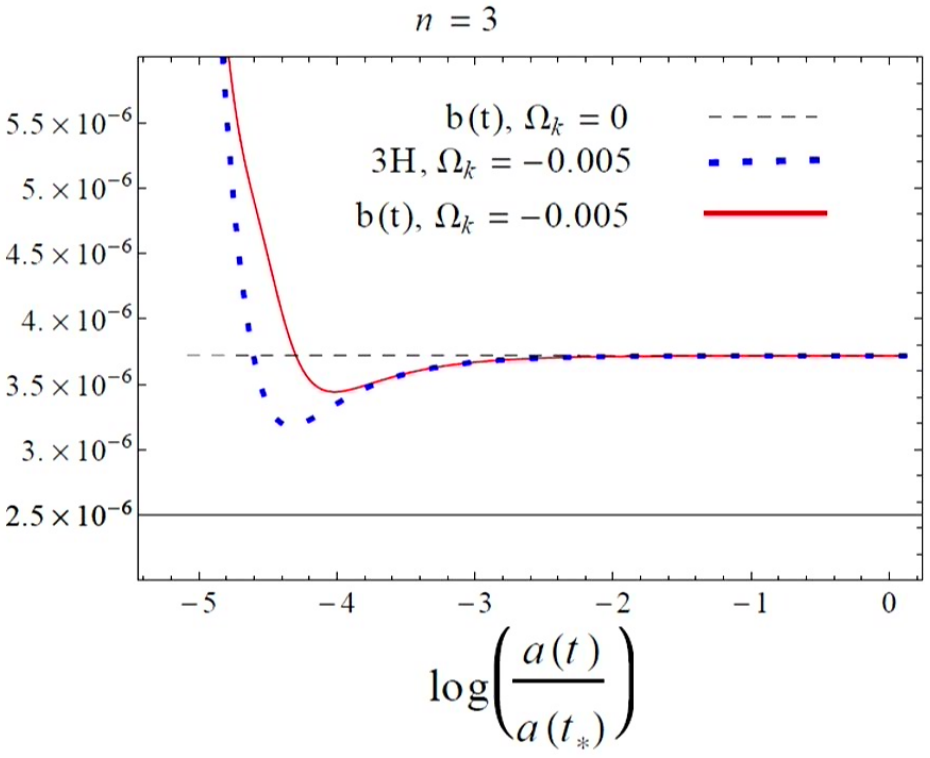

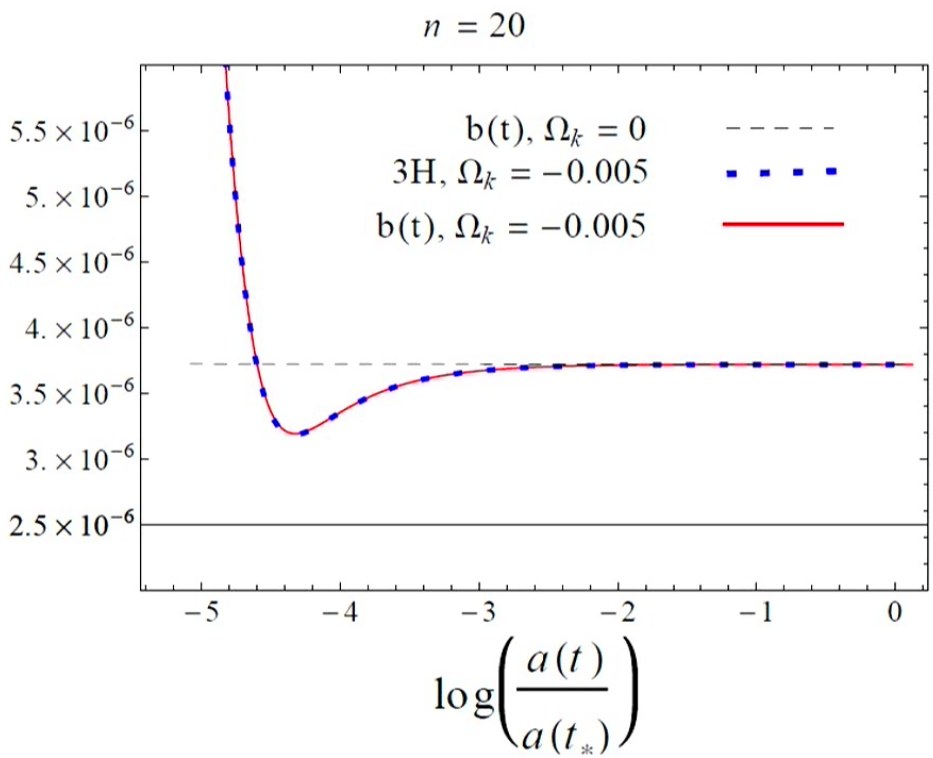

… and similarly for c(n,t)

Initial conditions perturbations

$$\ddot{q}_{nlm} + b(n,t)\dot{q}_{nlm} + c(n,t)q_{nlm} = 0$$

$$v_{nlm} = a\, q_{nlm}$$

$$v''_{nlm}(\eta) + \left(a\, b - 3\frac{a'}{a}\right) v'_{nlm} + \left[3\left(\frac{a'}{a}\right)^2 - \frac{a''}{a} - a'\, b + a^2\, c\right] v_{nlm} = 0$$

In static limit reduces to

$$v''_{nlm} + \underbrace{\left[m^2 a^2 \left(1 + \frac{6}{n^2-4}\left(1 + \frac{1}{a^2 H^2}\right)\right) + \frac{n^2-1}{r_o^2}\right]}_{\omega_n} v_{nlm} = 0$$

Instantaneous vacuum

$$v''_{nlm} + \omega_n v_{nlm} = 0$$

$$v_{nlm}(t_0) = \frac{1}{\sqrt{2\omega_n}} \qquad q_{nlm}(t_0) = \frac{1}{a_0\sqrt{2\omega_n}}$$

$$v'_{nlm}(t_0) = -i\sqrt{\frac{\omega_n}{2}} \qquad \dot{q}_{nlm}(t_0) = -\frac{\dot{a}_0}{a_0^2}\frac{1}{\sqrt{2\omega_n}} - \frac{i}{a_0^2}\sqrt{\frac{\omega_n}{2}}$$

Primordial power spectrum

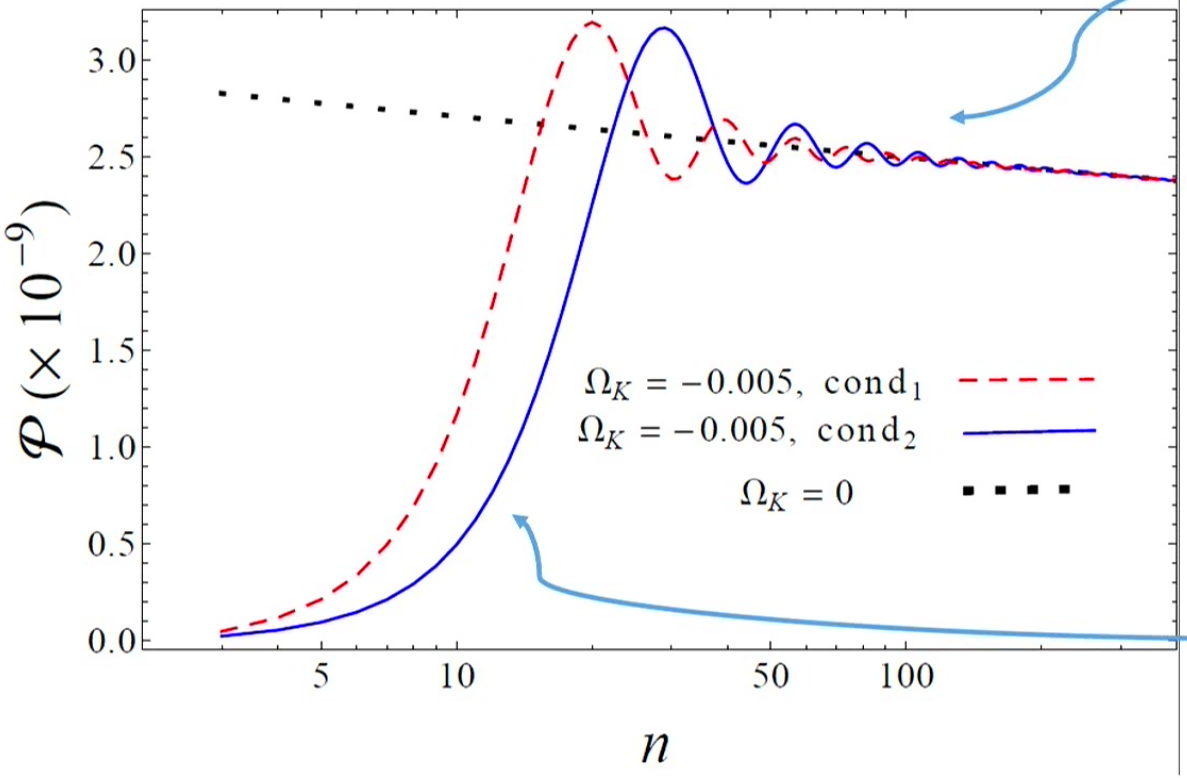

1 oscillatory power spectrum

2 $\mathcal{P}^{\mathrm{average}}_{\mathrm{closed}} < \mathcal{P}^{\mathrm{average}}_{\mathrm{flat}}$

CMB anisotropies

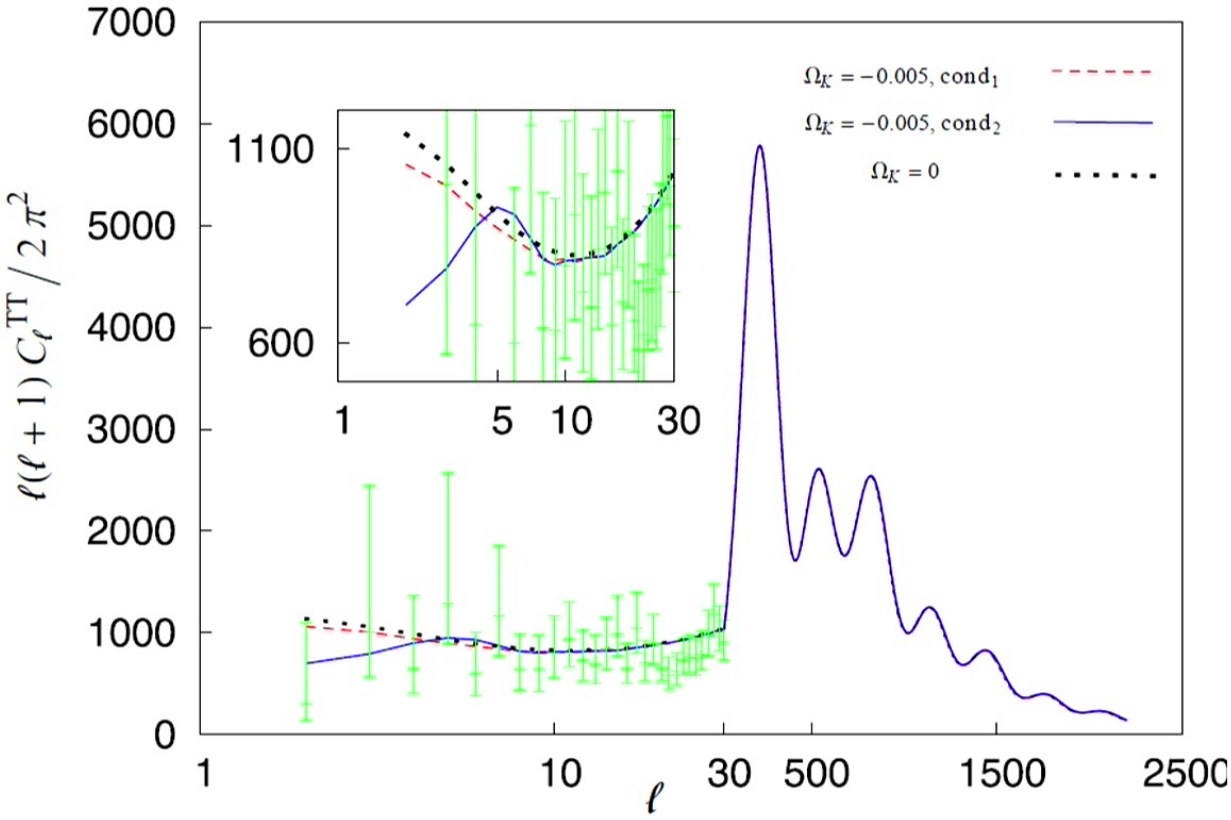

Parameter estimation

(*Planck+BAO+scale-invariant power spectrum*: $\Omega_K = 0.000^{+0.005}_{-0.005}$)

Parameters unchanged as modifications in temperature anisotropies are limited to low *l*'s

Summary

- Primordial power spectrum is altered at large scales
- However, resulting modifications in temperature anisotropies only for $l<10$
- Although in principle inconsistent, parameter estimation is robust

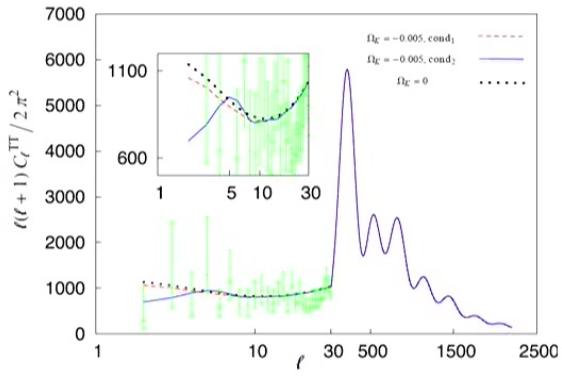

Outlook

- Investigate other CMB anomalies
- Tensor modes, B-mode polarization and consistency relation
- Extend to quantum gravity era
- Suggestions?

Spin-SILC: CMB polarisation component separation with spin wavelets

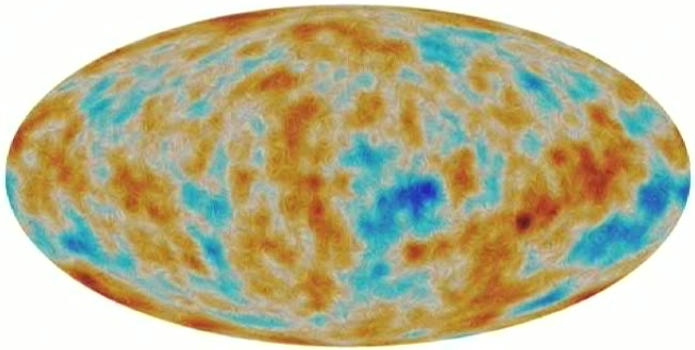

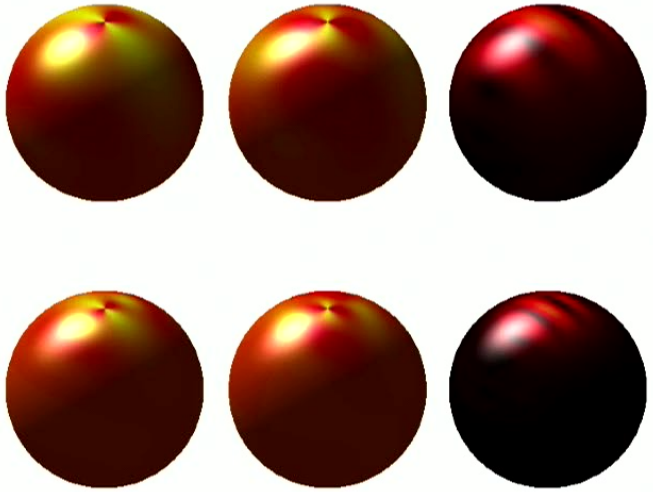

Keir K. Rogers

University College London

Promise of CMB *B*-mode polarisation

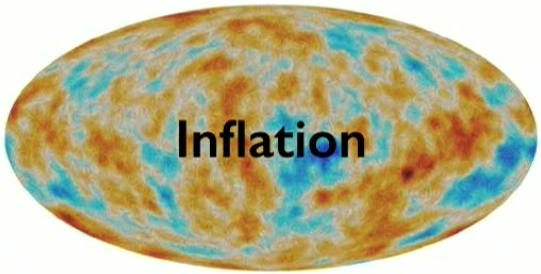

- Large international effort pursuing **primordial & lensing *B*-mode detections**
- Need improved data analysis to remove **polarised astrophysical foregrounds**
- Want to **coherently use all info in polarisation signal**

Planck Collaboration et al. (2015)

arxiv: 1601.01322, 1605.01417

K. Rogers, H. Peiris, B. Leistedt, J. McEwen, A. Pontzen, 2016, MNRAS, 460, 3014
& K. Rogers, H. Peiris, B. Leistedt, J. McEwen, A. Pontzen, 2016, MNRAS, submitted

with Hiranya Peiris[1], Boris Leistedt[2], Jason McEwen[1], Andrew Pontzen[1]

[1]University College London, [2]New York University

www.silc-cmb.org

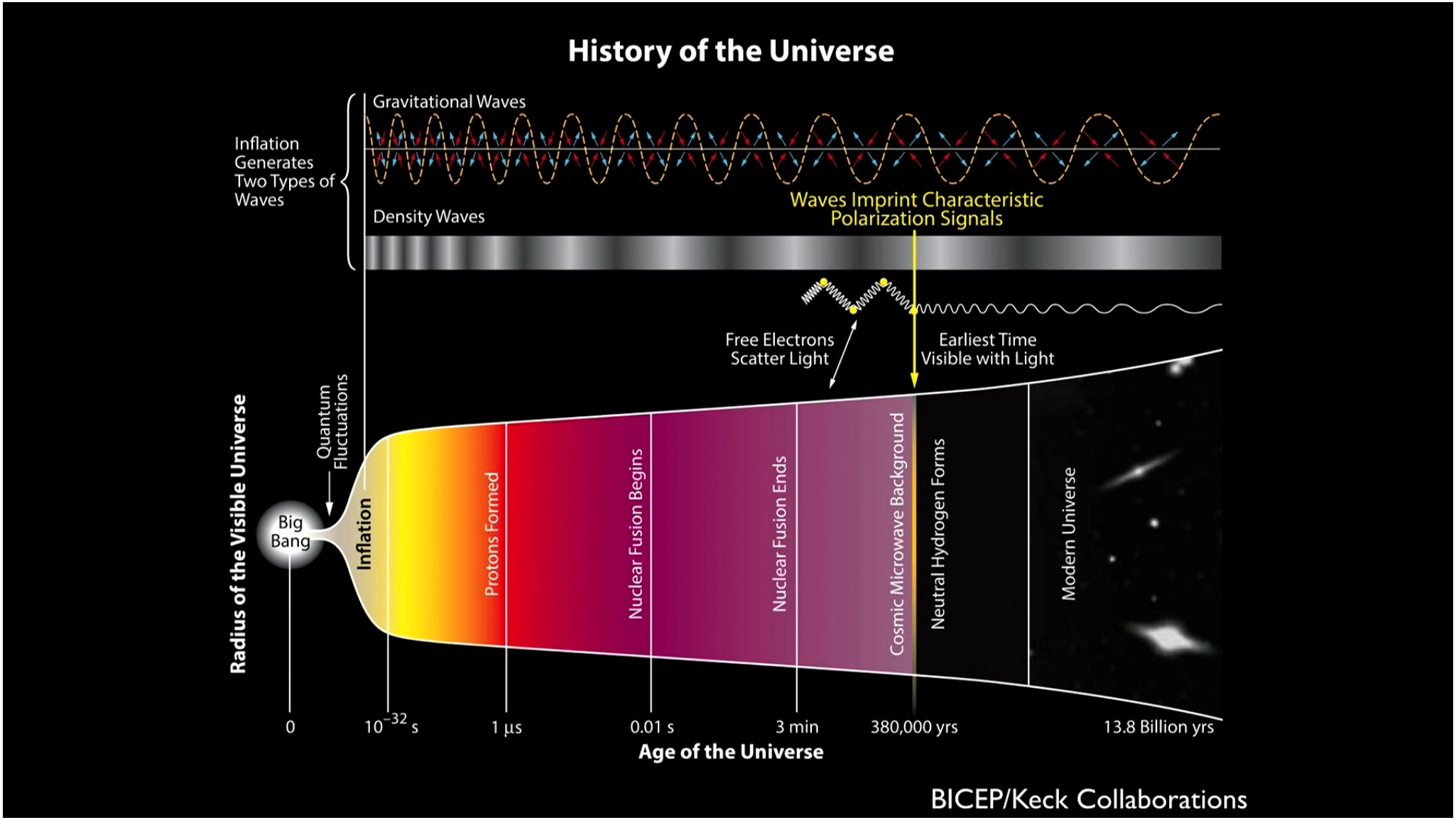
History of the Universe
Gravitational Waves
Inflation Generates Two Types of Waves
Density Waves
Waves Imprint Characteristic Polarization Signals
Free Electrons Scatter Light
Earliest Time Visible with Light
Quantum Fluctuations
Big Bang
Inflation
Protons Formed
Nuclear Fusion Begins
Nuclear Fusion Ends
Cosmic Microwave Background
Neutral Hydrogen Forms
Modern Universe
Radius of the Visible Universe
0
10−32 s
1 μs
0.01 s
3 min
380,000 yrs
13.8 Billion yrs
Age of the Universe
BICEP/Keck Collaborations

E & *B* modes produced by density & gravitational waves at last scattering surface

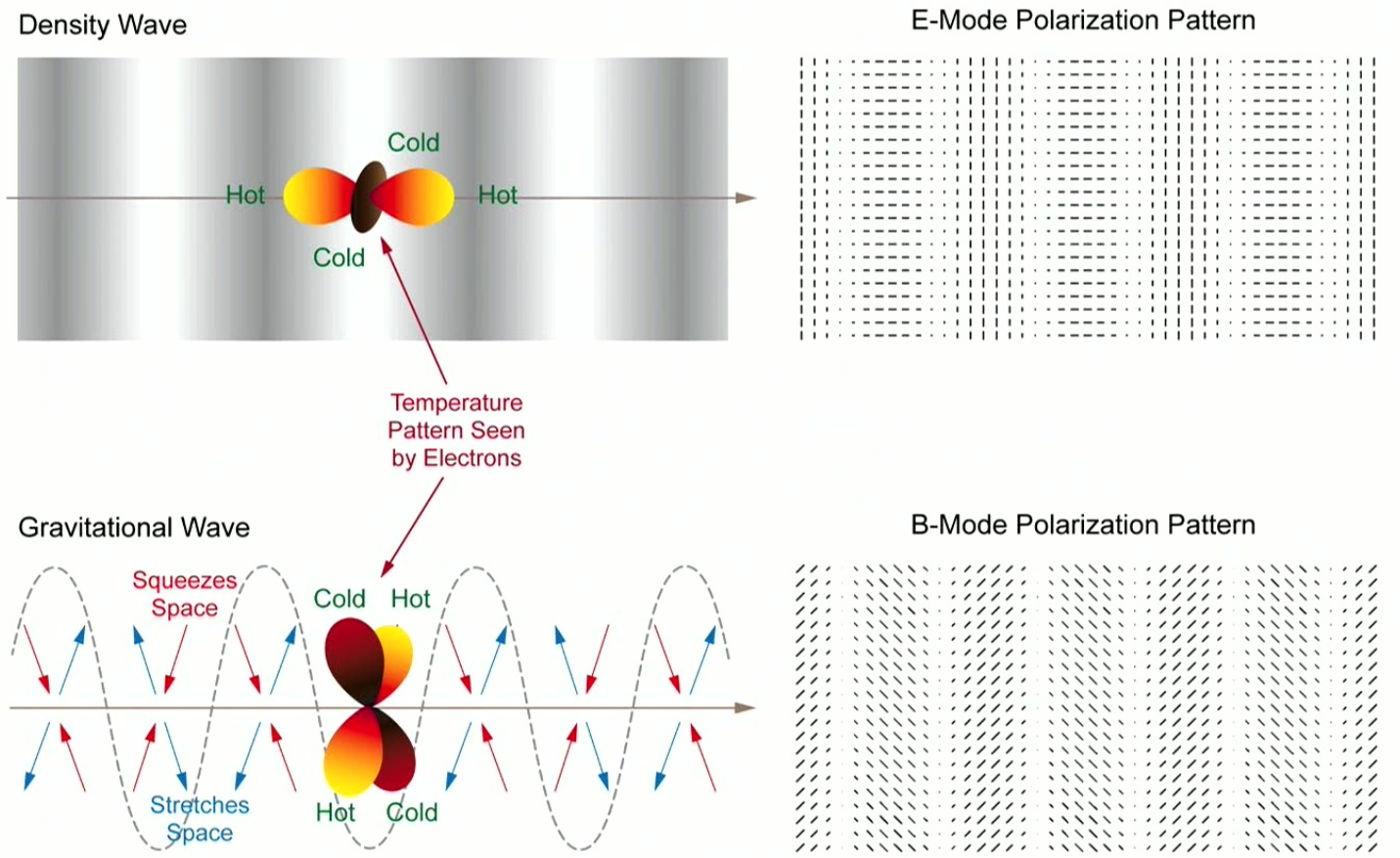

BICEP/Keck Collaborations

B modes also produced by weak lensing of *E* modes

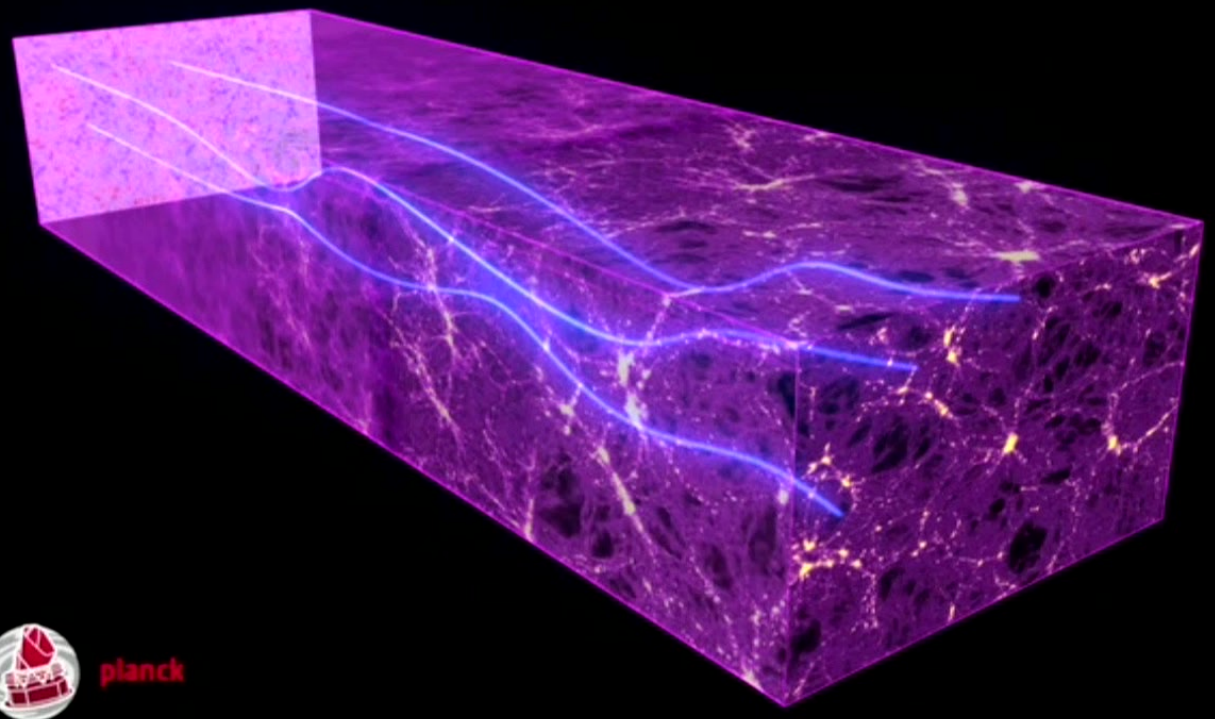

planck

ESA/Planck Collaboration

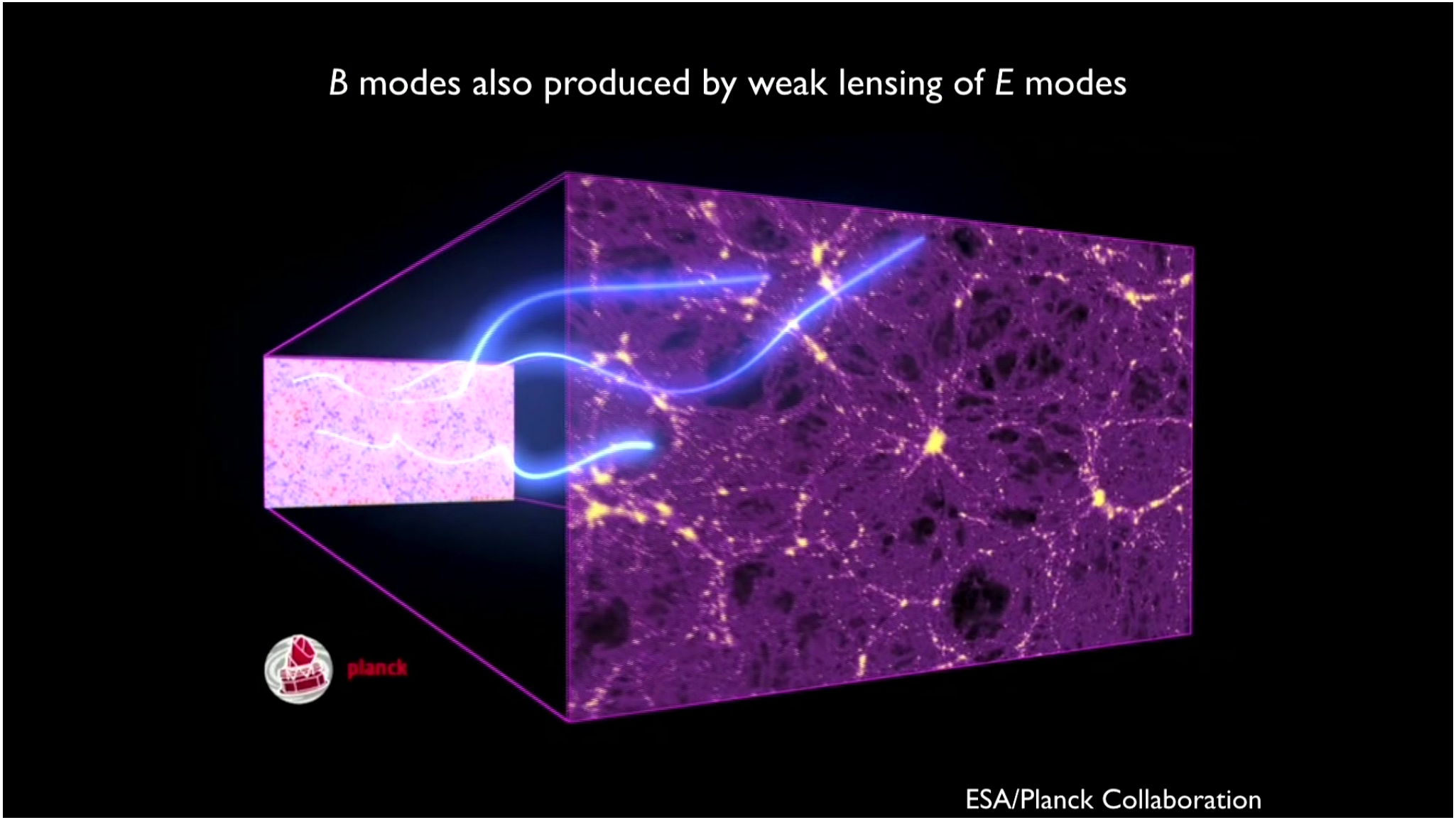
B modes also produced by weak lensing of E modes
planck
ESA/Planck Collaboration

Measure microwave sky at multiple frequencies to disentangle cosmology from astrophysics

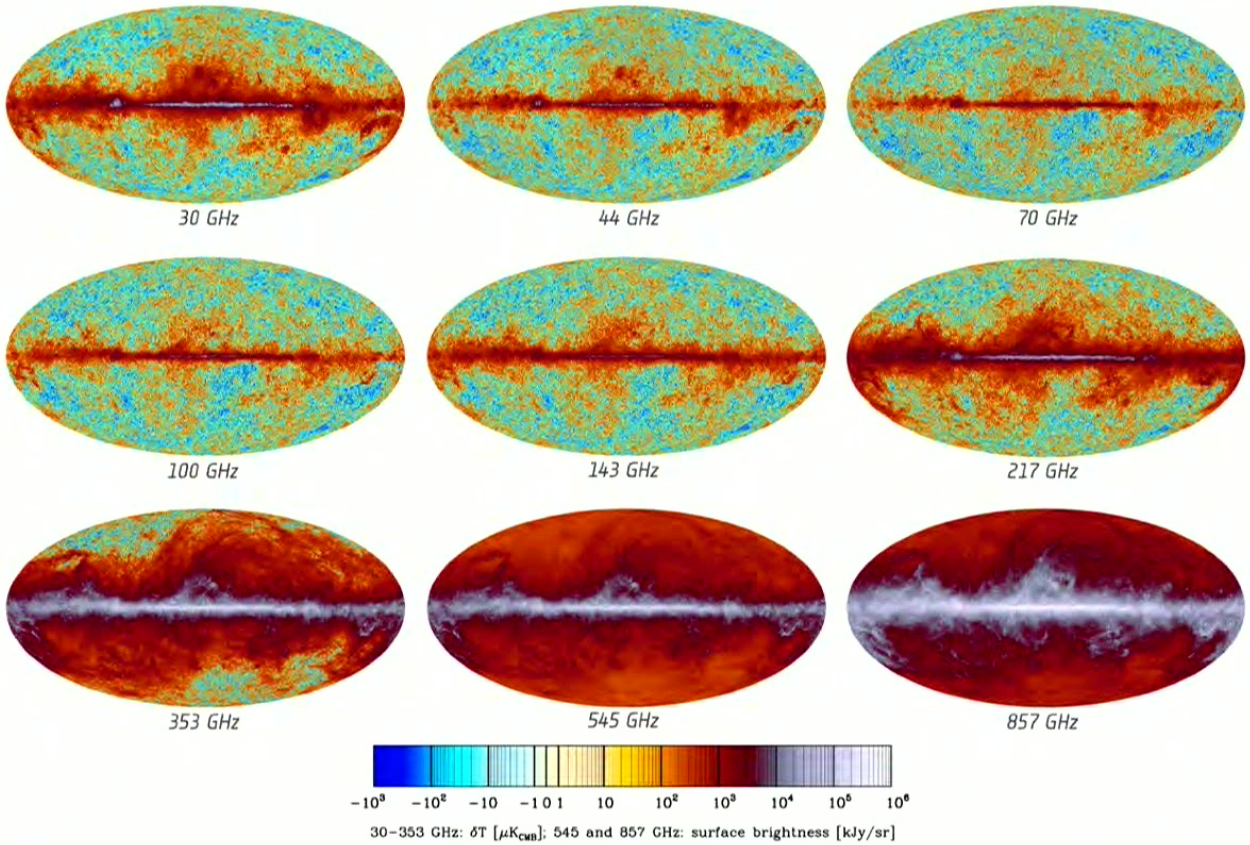

Planck Collaboration et al. (2014)

Planck Temperature & *E*-Mode Polarisation

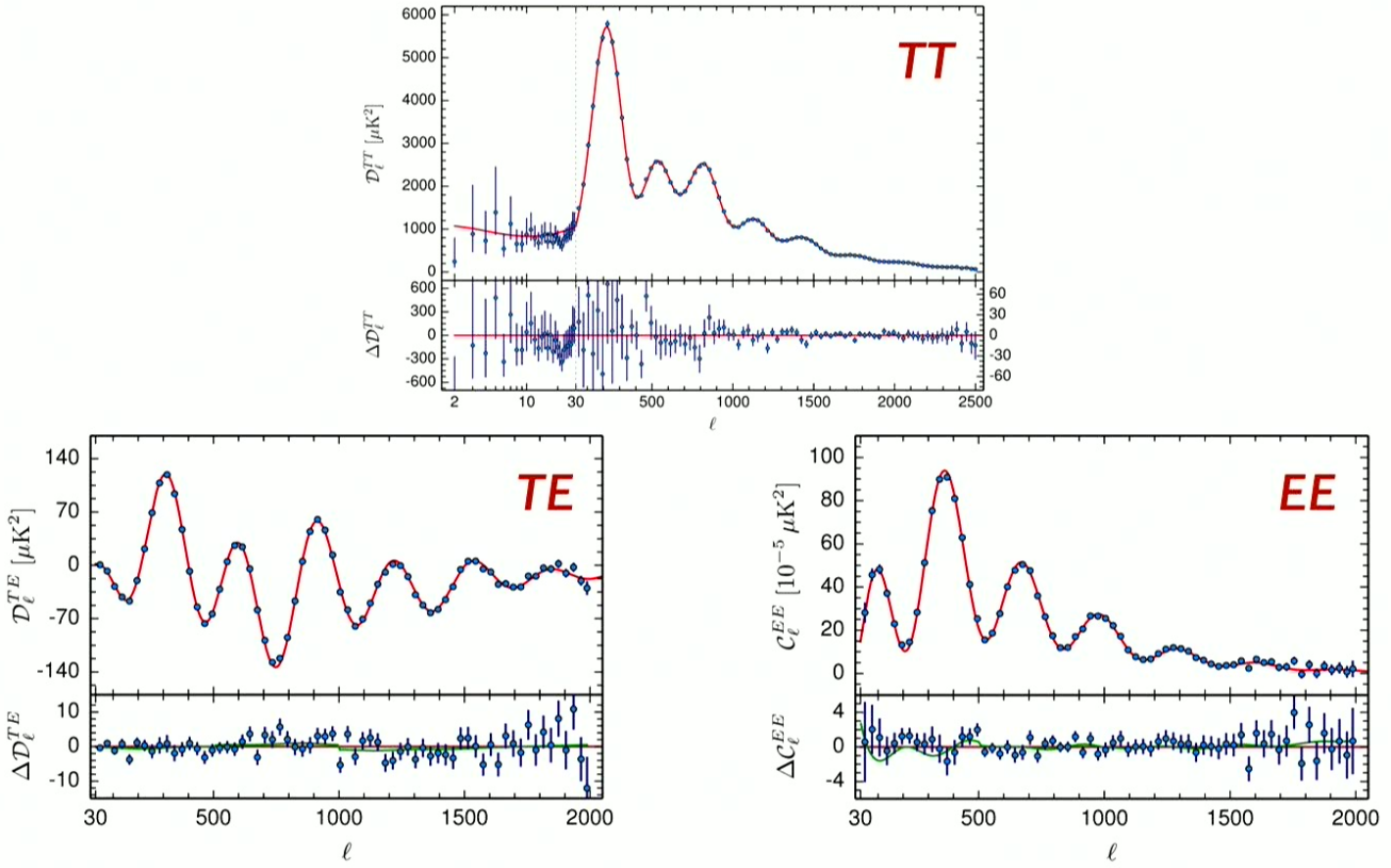

Planck Collaboration et al. (2015)

Challenges of *B*-Mode Detection

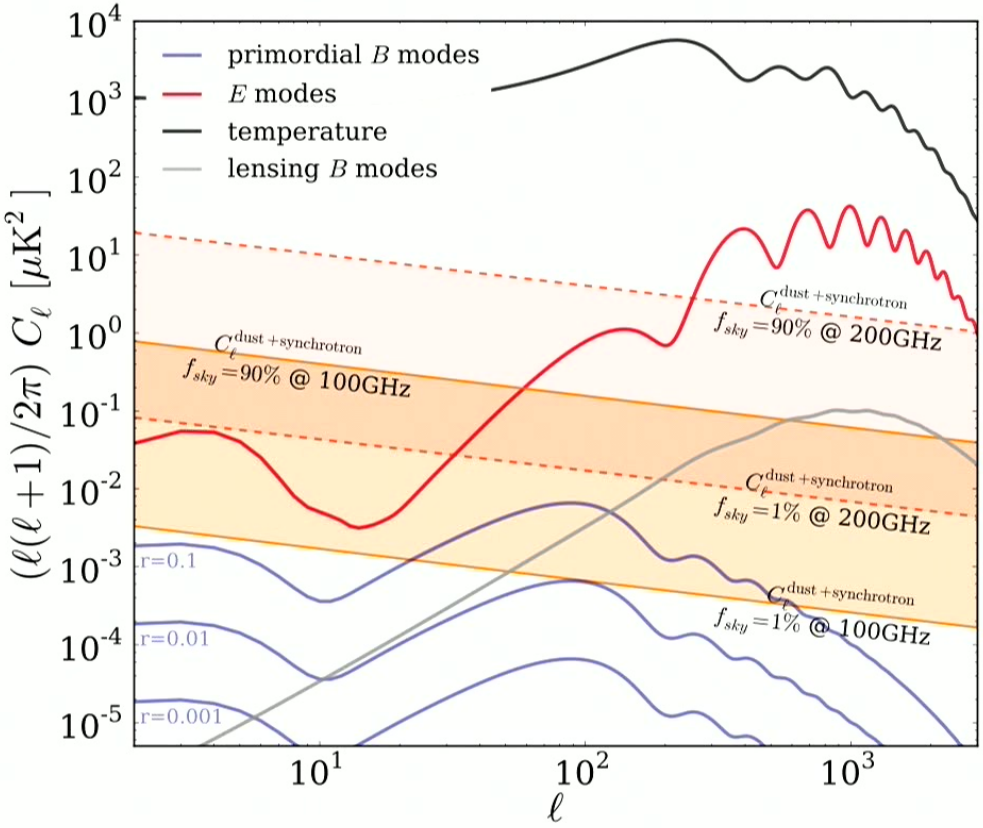

Errard & Feeney, et al. (2016)

Observational Status of *B* Modes

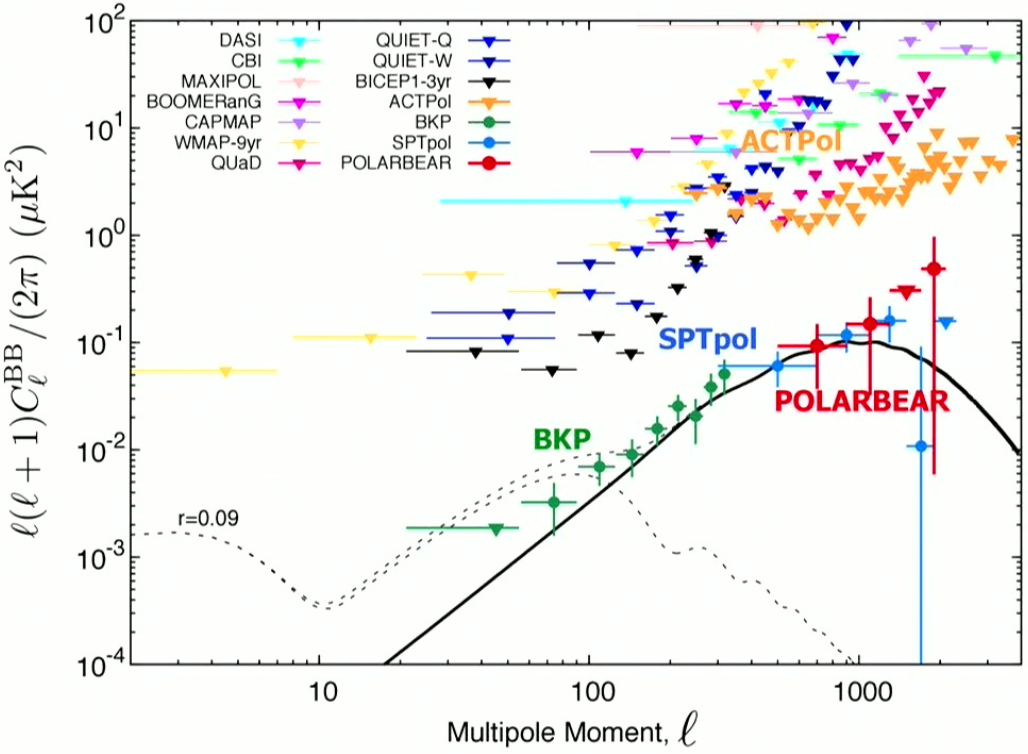

A Measurement of the Cosmic Microwave Background *B*-Mode Polarization Power Spectrum at Sub-Degree Scales with POLARBEAR
The POLARBEAR Collaboration
The Astrophysical Journal (2014)

Measurements of Sub-Degree *B*-Mode Polarization in the Cosmic Microwave Background from 100 Square Degrees of SPTpol Data
R. Keisler et al.
The Astrophysical Journal (2015)

Joint Analysis of BICEP 2 / Keck Array and *Planck* Data
P. Ade et al.
Physical Review Letters (2015)

BICEP/Keck Array 95 GHz (2015)
$r < 0.09$ (95%)

Josquin Errard

Observational Status of *B* Modes

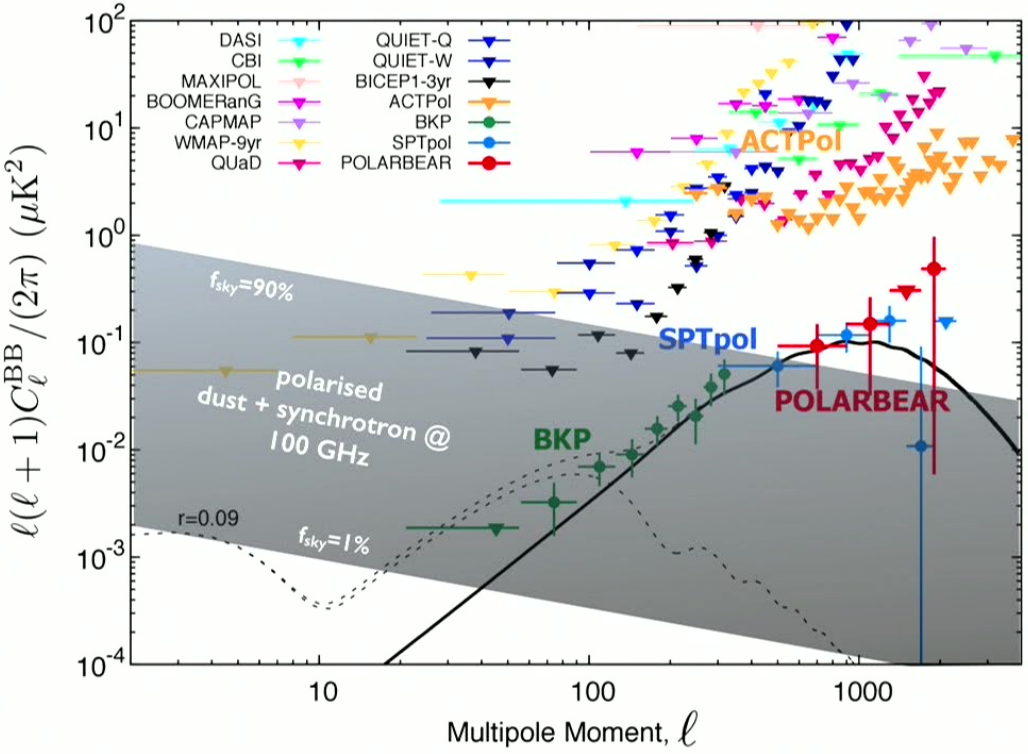

A Measurement of the Cosmic Microwave Background *B*-Mode Polarization Power Spectrum at Sub-Degree Scales with POLARBEAR
The POLARBEAR Collaboration
The Astrophysical Journal (2014)

Measurements of Sub-Degree *B*-Mode Polarization in the Cosmic Microwave Background from 100 Square Degrees of SPTpol Data
R. Keisler et al.
The Astrophysical Journal (2015)

Joint Analysis of BICEP 2 / Keck Array and *Planck* Data
P. Ade et al.
Physical Review Letters (2015)

BICEP/Keck Array 95 GHz (2015)
$r < 0.09$ (95%)

Josquin Errard

Pre-2020 *B*-mode experiments x *Planck* can get $\sigma(r) \sim 3 \times 10^{-3}$

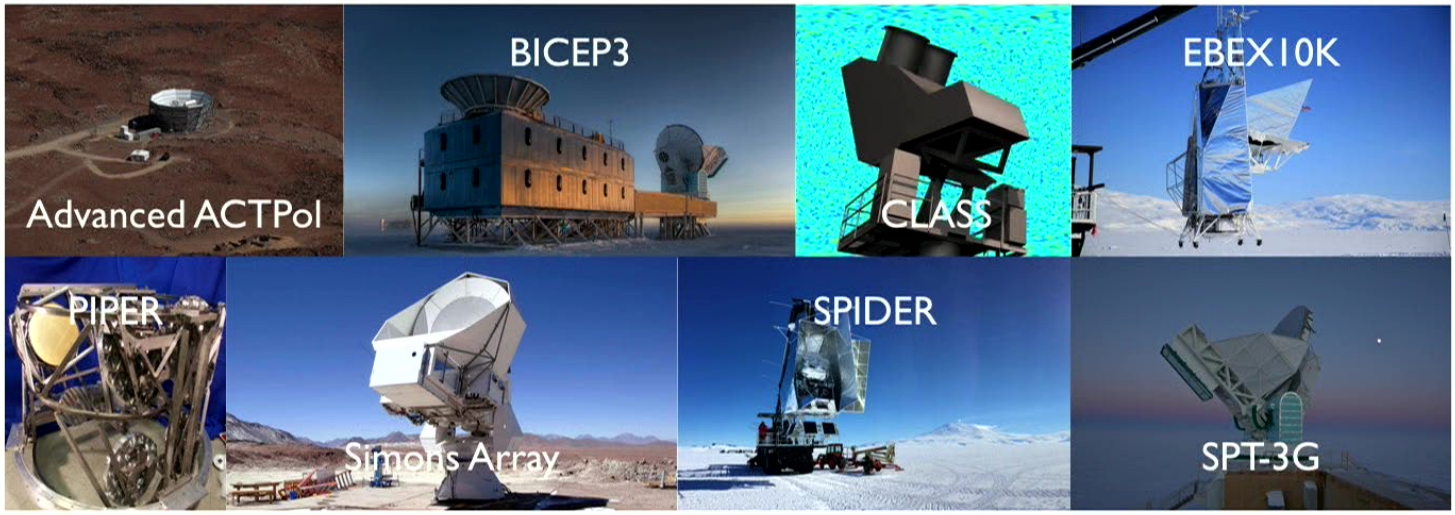

Post-2020 *B*-mode experiments could get $\sigma(r) \sim 1.3 \times 10^{-4}$

CORE++ (Stage-V?)

LiteBIRD-ext

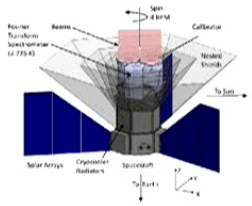

PIXIE

Stage-IV CMB?

Errard & Feeney, et al. (2016)

Polarised Astrophysical Foregrounds

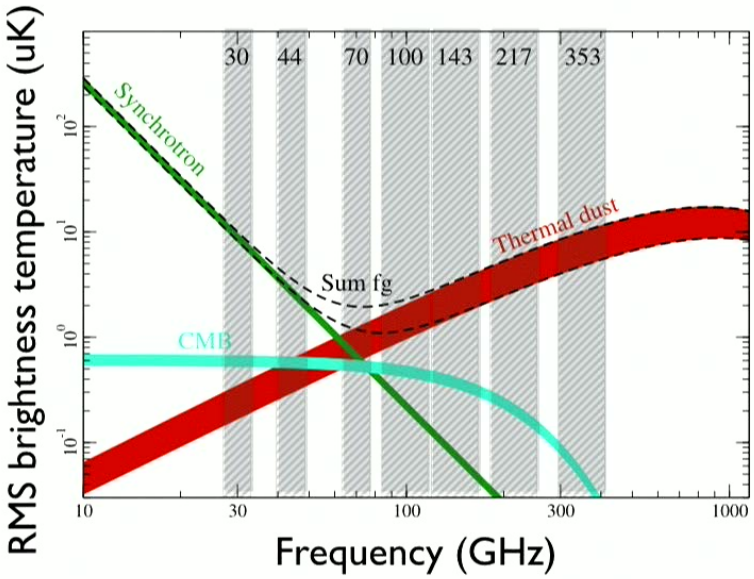

Spectra

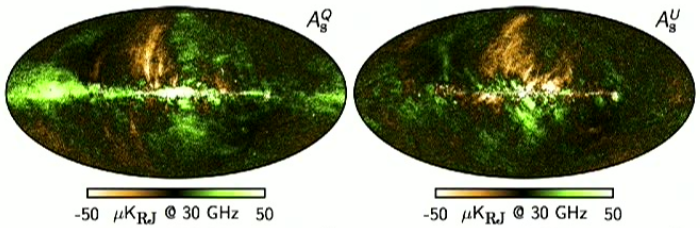

Maps

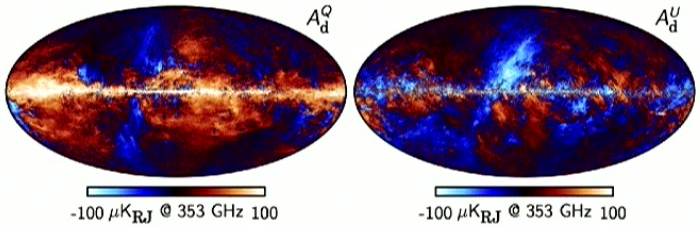

Planck Collaboration et al. (2015)

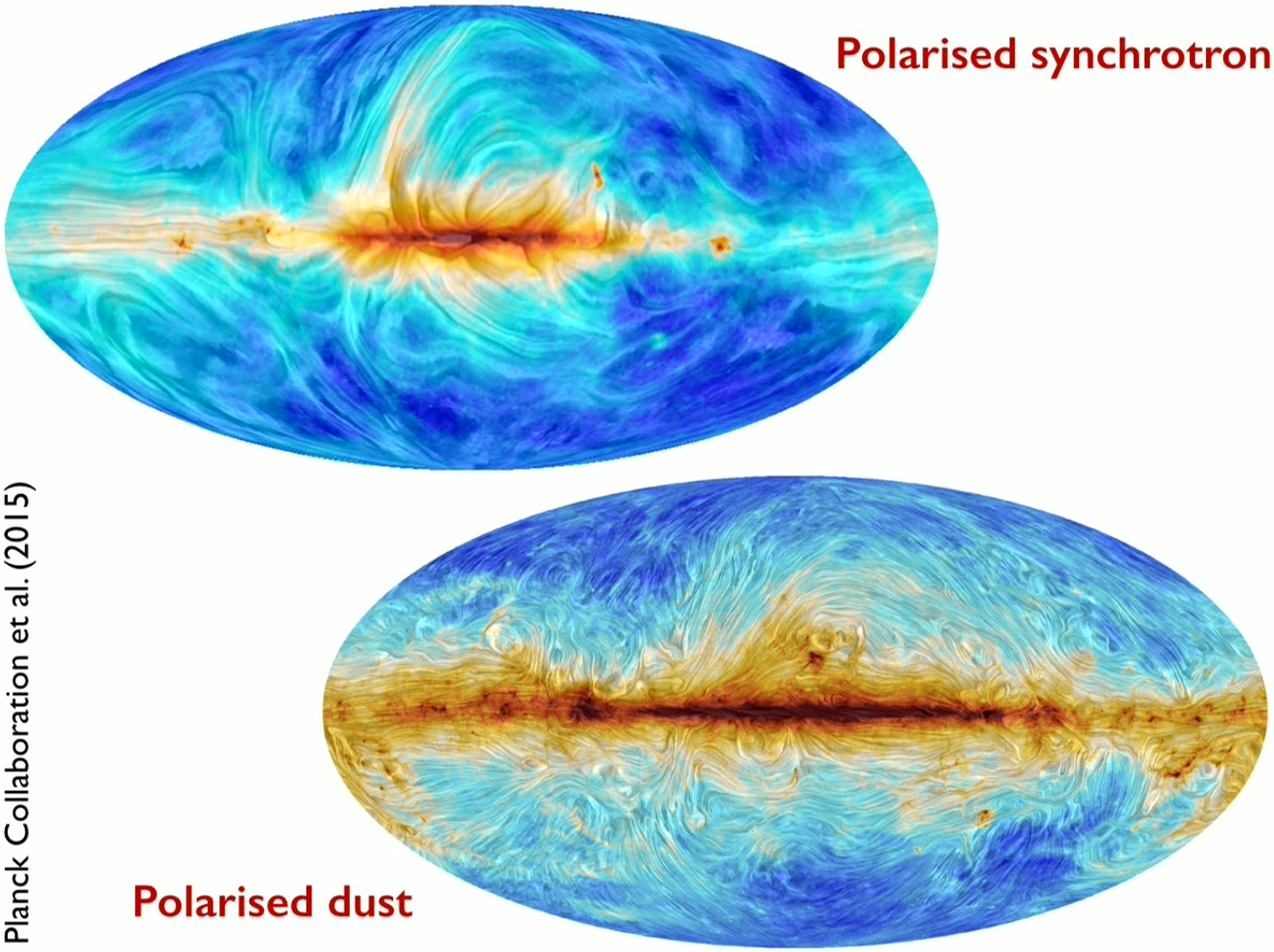
Polarised synchrotron
Planck Collaboration et al. (2015)
Polarised dust

E - *B* Mode Decomposition

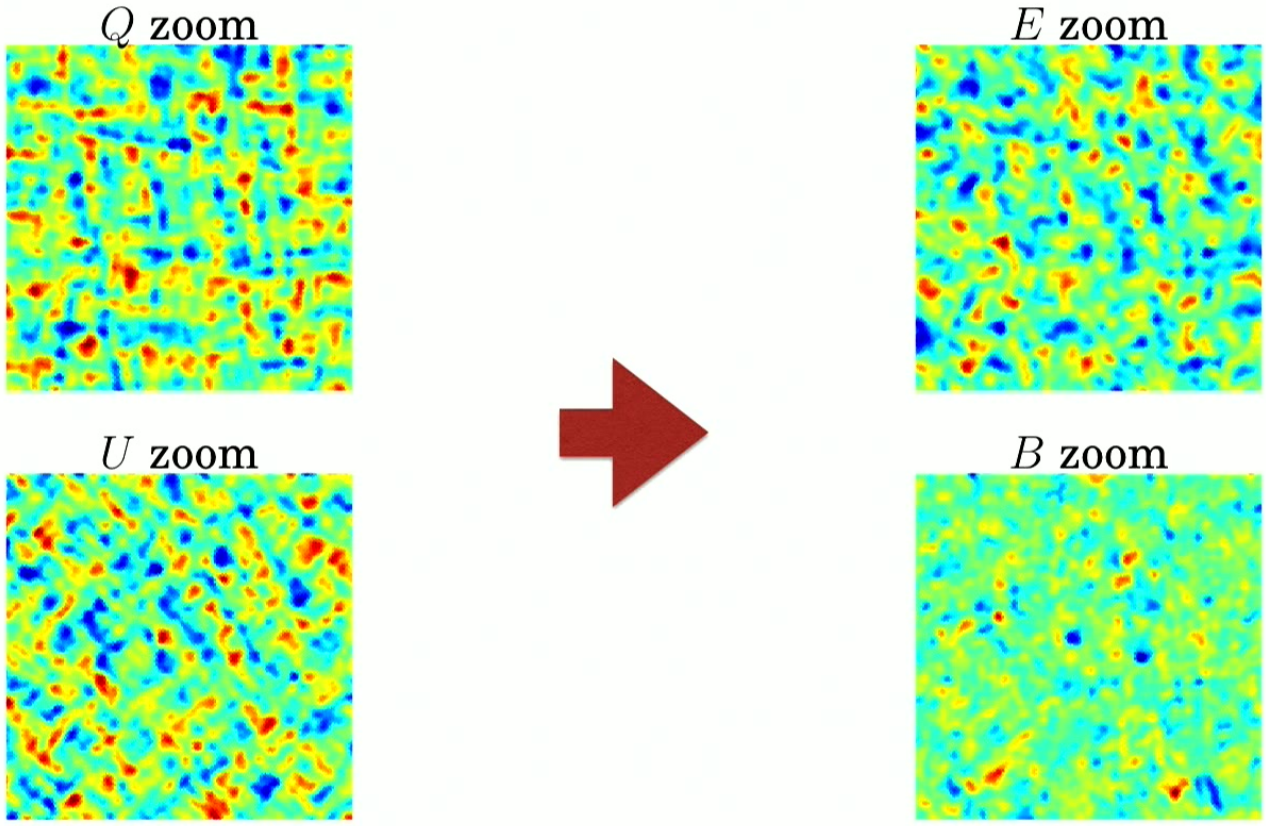

Internal Linear Combination

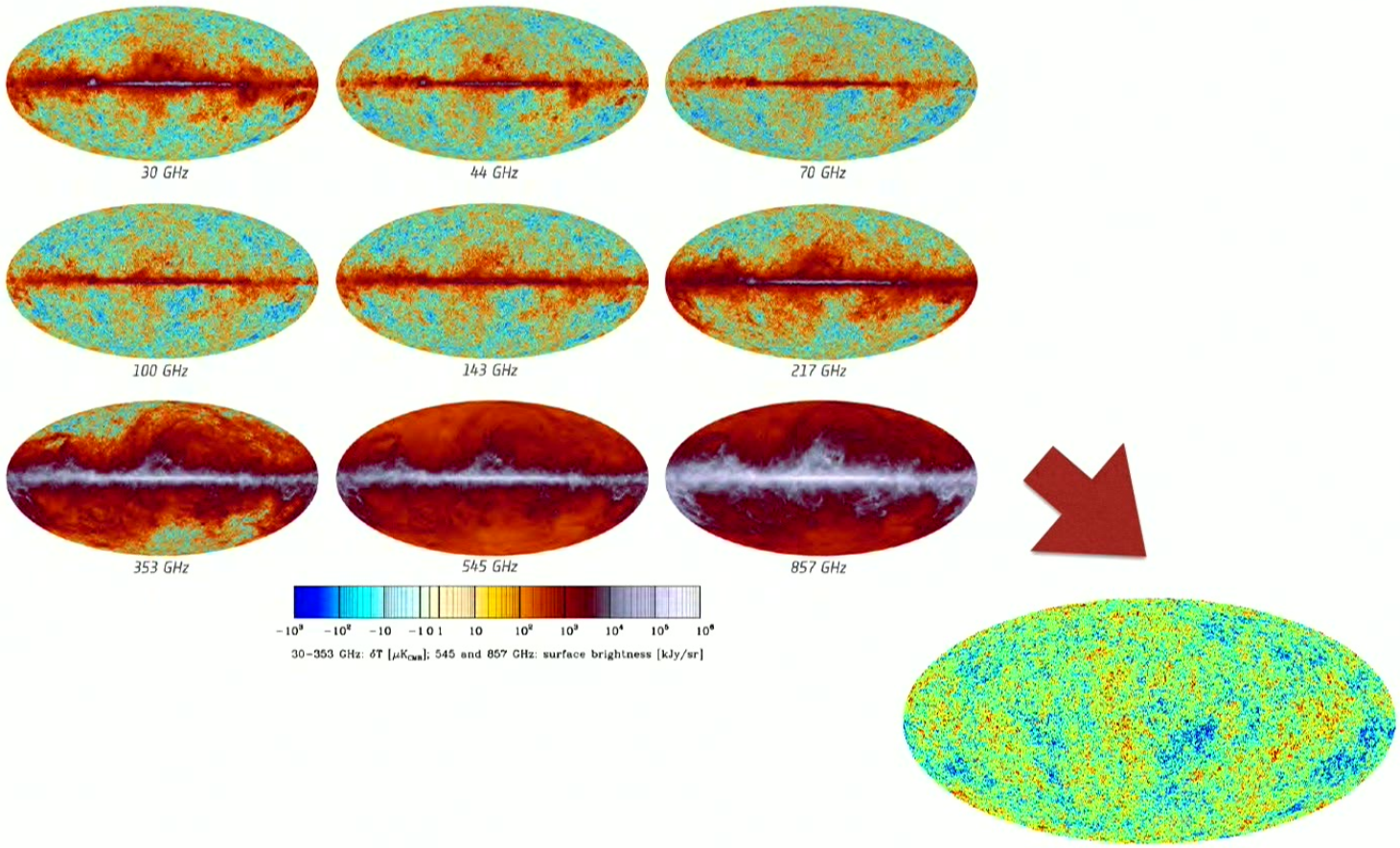

Planck Collaboration et al. (2014)

Internal Linear Combination: Details

Data model

$$T_p^c = T_p^{\mathrm{CMB}} + T_p^{\mathrm{FG},c} + T_p^{\mathrm{N},c}$$

ILC is constrained linear sum

$$T_p^{\mathrm{ILC}} = \sum_c \omega_p^c T_p^c$$

Constraint conserves CMB

$$\sum_c \omega_p^c = 1 \implies T_p^{\mathrm{ILC}} = T_p^{\mathrm{CMB}} + T_p^{\mathrm{res}}$$

ILC defined to minimise output variance

$$\mathrm{E}({T_p^{\mathrm{ILC}}}^2) = \mathrm{E}({T_p^{\mathrm{CMB}}}^2) + \mathrm{E}(T_p^{\mathrm{res}2}) + \mathrm{E}(T_p^{\mathrm{CMB}} T_p^{\mathrm{res}})$$

Developing Localisation of ILC Weights

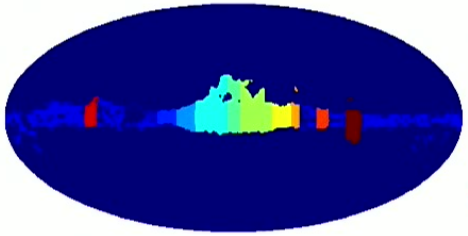

Spatial

WMAP Collab. (2003)

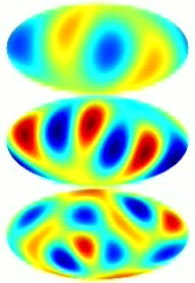

Harmonic

Tegmark et al. (2003)

NILC

+ Morphological

SILC

+ Spin

Spin-SILC

NILC: Delabrouille et al. (2009)
(Spin-)SILC: Rogers et al. (2016a,b)
Wang et al. (2015)

Axisymmetric Wavelets

Wavelets: localised in both real & harmonic space

$$\Psi^j(\theta,\phi) = \sum_{\ell m} \Psi^j_{\ell m} Y_{\ell m}(\theta,\phi)$$

$$\Psi^j_{\ell m} \equiv \sqrt{\tfrac{2\ell+1}{4\pi}}\,\kappa^j(\ell)\,\delta_{m0}$$

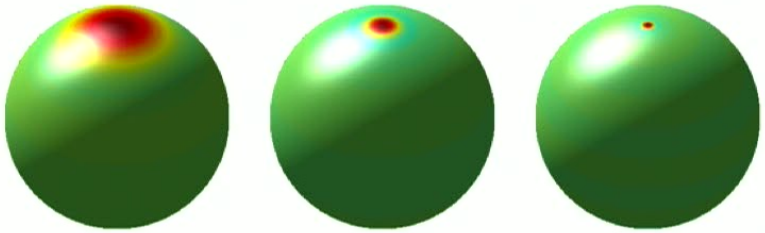

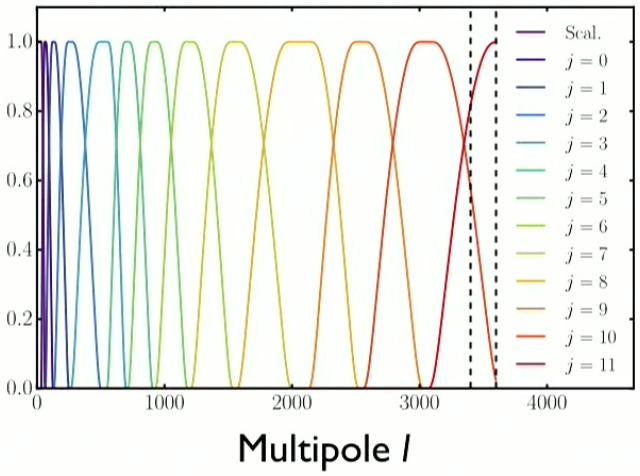

Spatial localisation

Harmonic localisation

Wiaux et al. (2009)
Leistedt et al. (2012)

Directional Wavelets

Wavelets: localised in real, harmonic & "directional" space

$$\Psi^j(\theta,\phi) = \sum_{\ell m} \Psi^j_{\ell m} Y_{\ell m}(\theta,\phi)$$

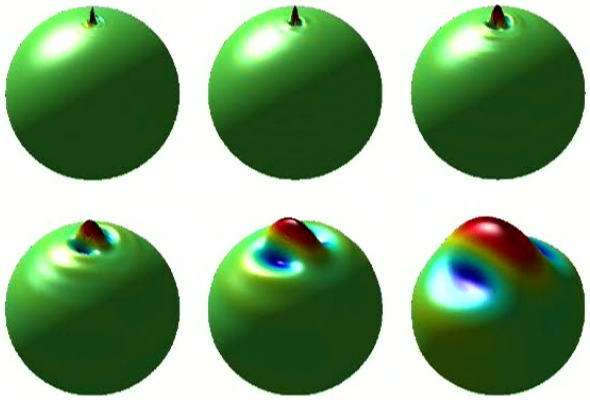

Spatial localisation

$$\Psi^j_{\ell m} \equiv \sqrt{\tfrac{2\ell+1}{8\pi^2}}\,\kappa^j(\ell)\, s_{\ell m}$$

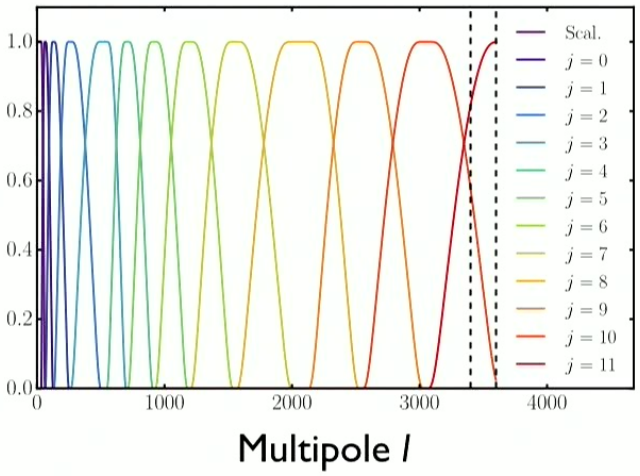

Harmonic localisation

McEwen et al. (2013)

Directional Wavelet Convolution

Bond & Efstathiou (1987) - CMB spots anisotropic

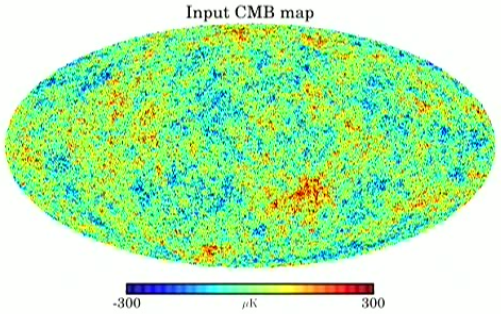

Directional localisation

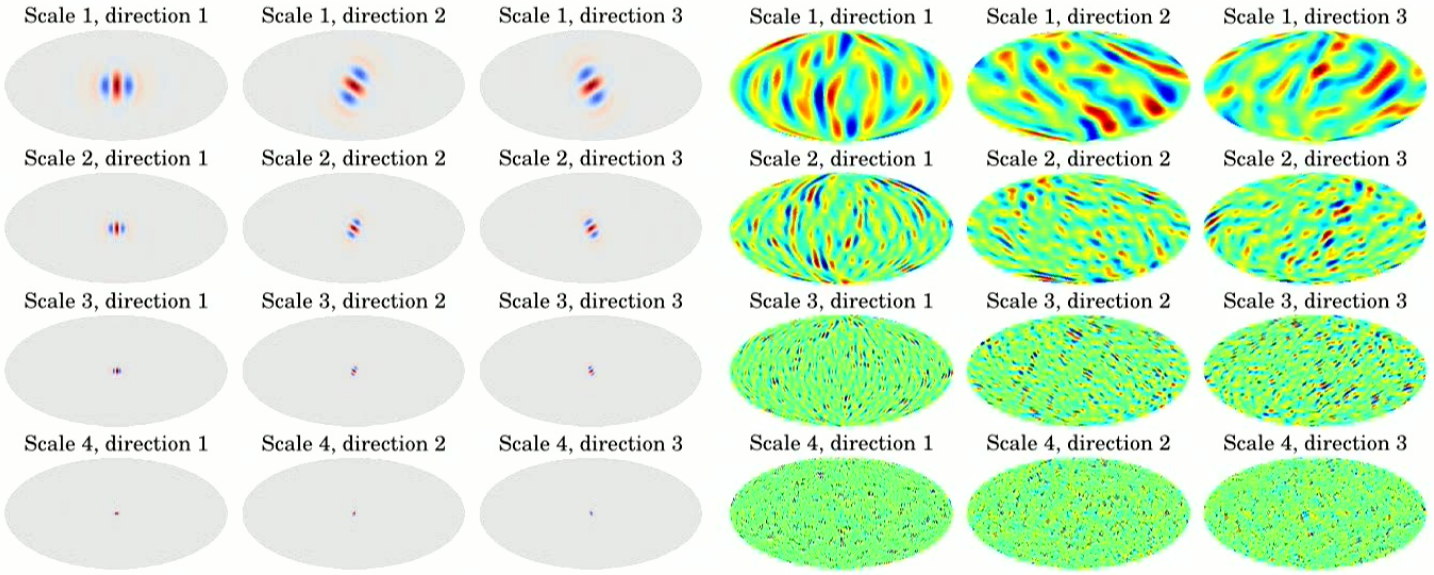

Spin Directional Wavelets

Wavelets: localised in real, harmonic & "directional" space

$$ {}_2\Psi^j(\theta,\phi) = \sum_{\ell m} {}_2\Psi^j_{\ell m}\, {}_2Y_{\ell m}(\theta,\phi) \qquad {}_2\Psi^j_{\ell m} \equiv \sqrt{\frac{2\ell+1}{8\pi^2}}\,\kappa^j_\ell\, {}_2s_{\ell m} $$

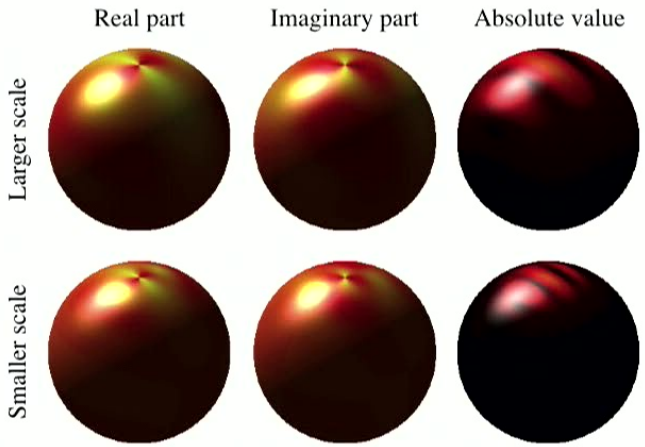

Spatial localisation

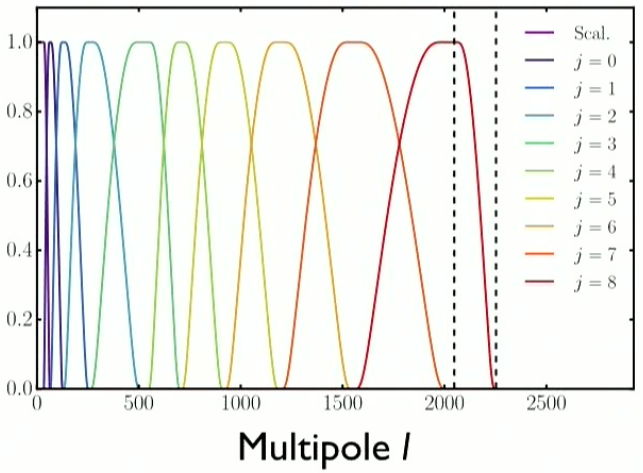

Harmonic localisation

McEwen et al. (2015)

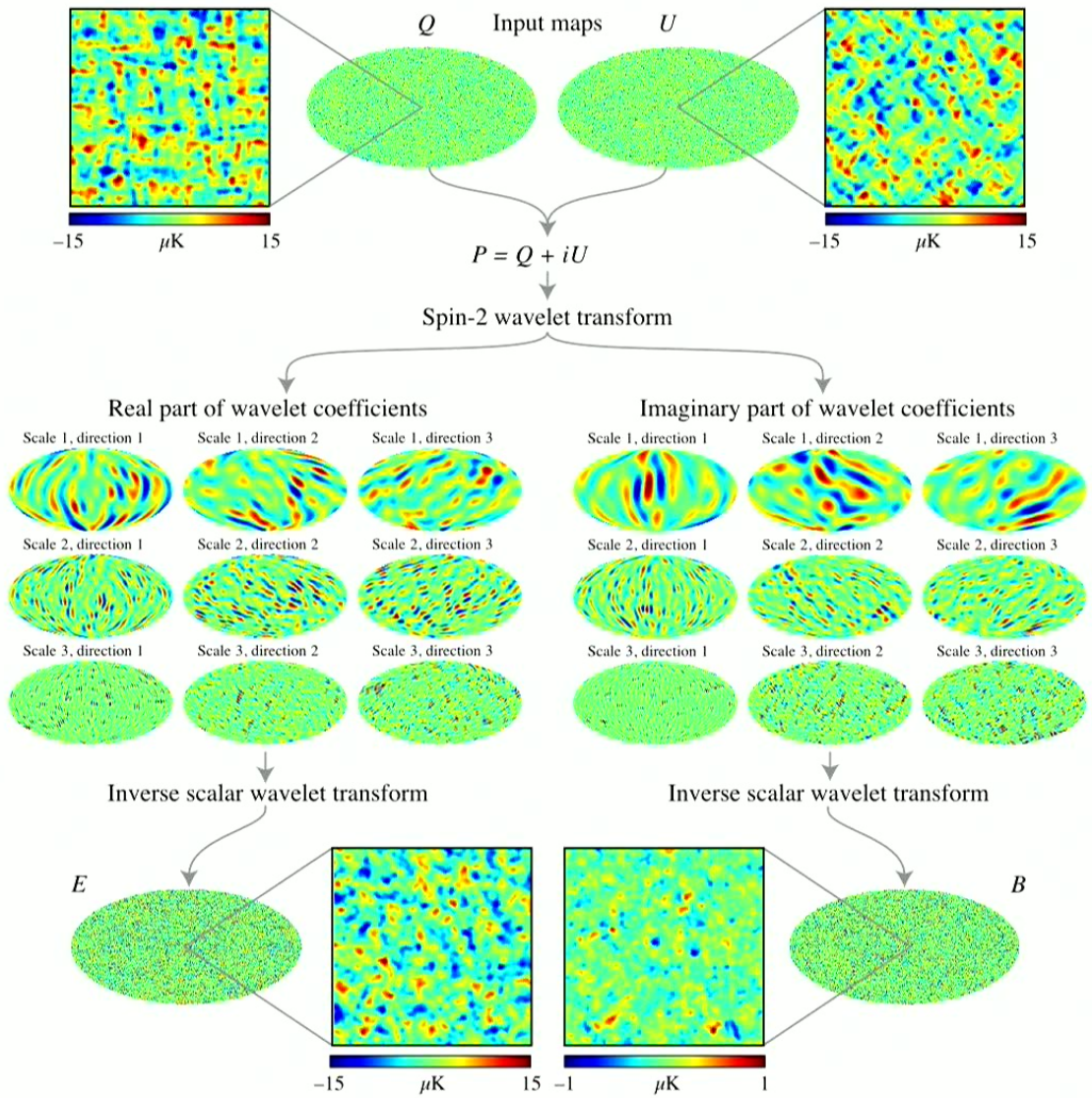
Q
Input maps
U
−15
μK
15
−15
μK
15
P = Q + iU
Spin-2 wavelet transform
Real part of wavelet coefficients
Imaginary part of wavelet coefficients
Scale 1, direction 1
Scale 1, direction 2
Scale 1, direction 3
Scale 2, direction 1
Scale 2, direction 2
Scale 2, direction 3
Scale 3, direction 1
Scale 3, direction 2
Scale 3, direction 3
Scale 1, direction 1
Scale 1, direction 2
Scale 1, direction 3
Scale 2, direction 1
Scale 2, direction 2
Scale 2, direction 3
Scale 3, direction 1
Scale 3, direction 2
Scale 3, direction 3
Inverse scalar wavelet transform
Inverse scalar wavelet transform
E
B
−15
μK
15
−1
μK
1

Testing on *Planck* Simulations & Data

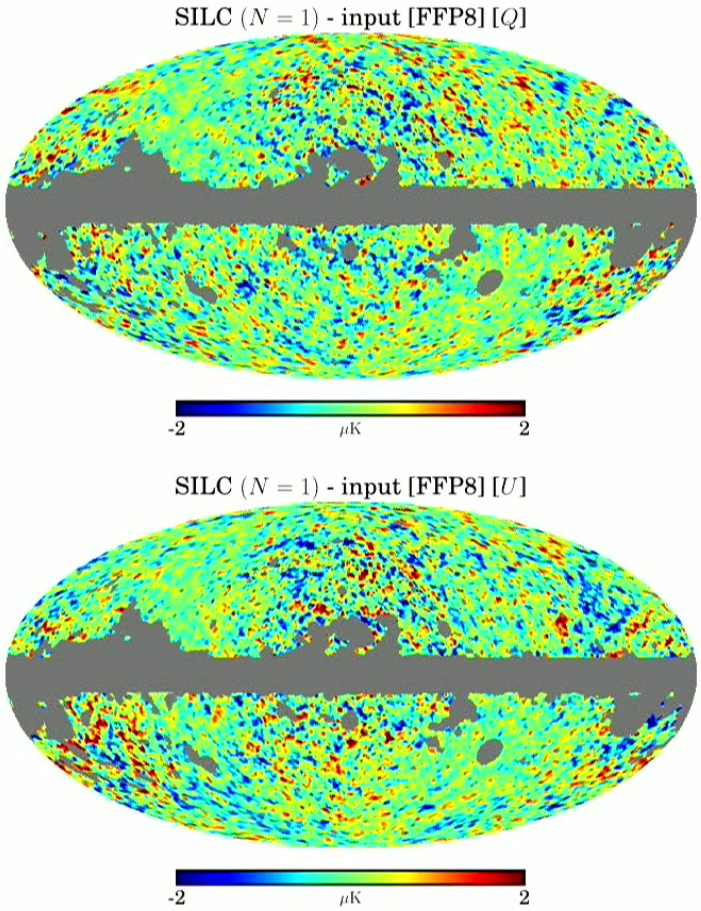

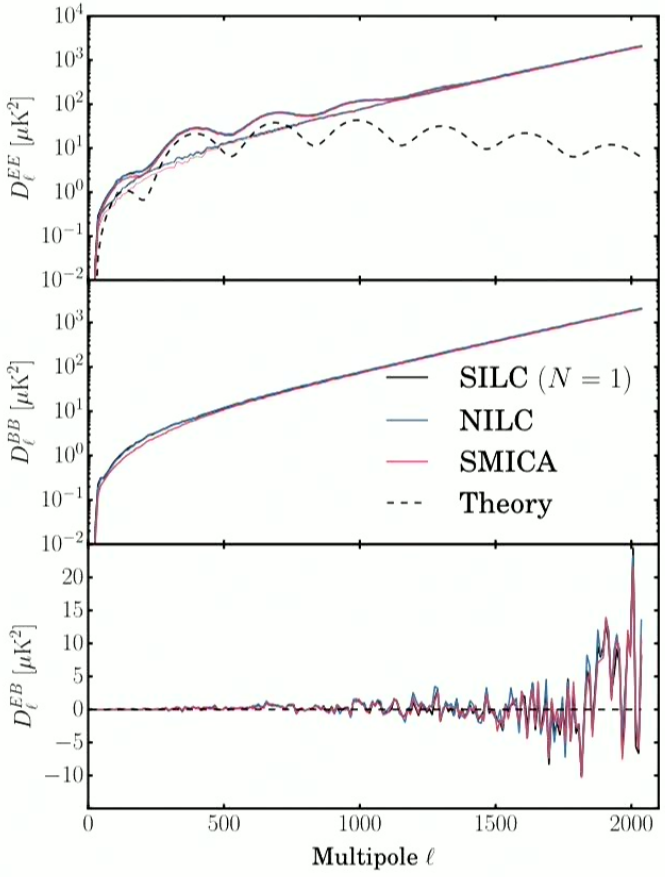

Future Applications of Spin-SILC

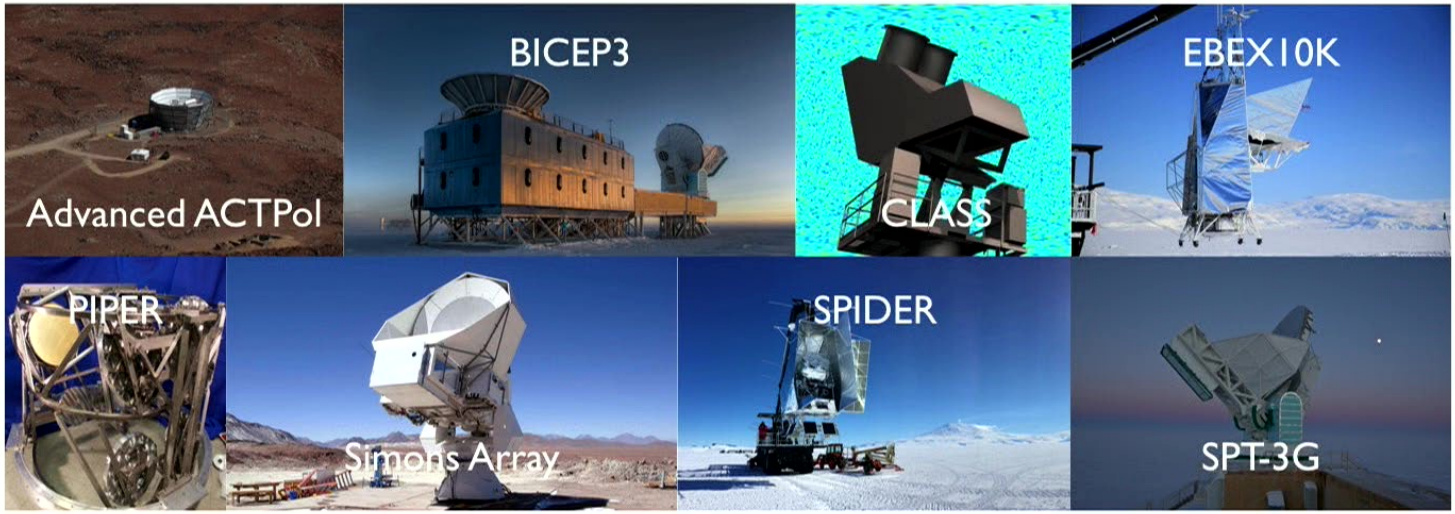

E-B mode leakage problem on partial-sky data

Combine Spin-SILC with **spin wavelet pure mode map estimator**

Lewis et al. (2002); Bunn et al. (2003);
Smith & Zaldarriaga (2007); Grain et al. (2012); Ferté et al. (2013); Leistedt et al. (2016)

Future Applications of Spin-SILC

Sunyaev-Zeldovich effect

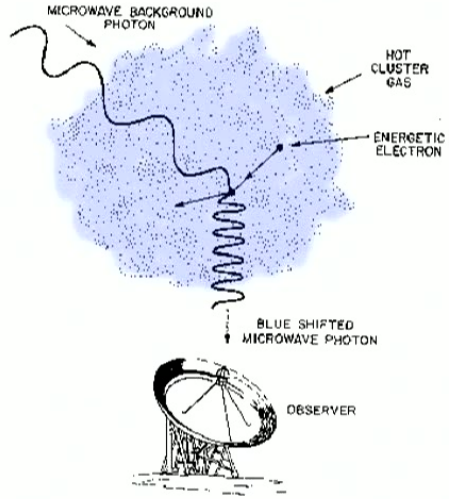

thermal Sunyaev-Zeldovich (tSZ) effect >> kinetic Sunyaev-Zeldovich (kSZ) effect

Generalise ILC to additionally cancel tSZ effect

Get clean **kSZ maps for cross-correlation** with large scale structure data

Summary

- Spin-SILC: advanced blind component separation / *E*-*B* decomposition method
- Designed for next generation high sensitivity polarisation data
- arxiv: 1601.01322, 1605.01417 — www.silc-cmb.org

E zoom

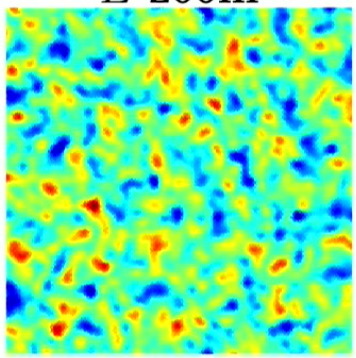

B zoom